A K M Monsurul Alam

Design and Analysis of a Wideband Feed for Metsähovi Compact Array

School of Electrical Engineering

Thesis submitted for examination for the degree of Master of Science in Technology.

Espoo 23.01.2017

Thesis supervisor:

Prof. Anne Lähteenmäki

Thesis advisor:

Petri Kirves M.Sc. (Tech.)

Aalto University
School of Electrical
Engineering

AALTO UNIVERSITY
SCHOOL OF ELECTRICAL ENGINEERING

ABSTRACT OF THE
MASTER'S THESIS

Author: A K M Monsurul Alam

Title: Design and Analysis of a Wideband Feed for Metsähovi Compact Array

Date: 23.01.2017 Language: English Number of pages:6+56

Department of Electronics and Nanoengineering

Professorship: Radio Astronomy Code: ELEC 3029

Supervisor: Prof. Anne Lähteenmäki

Advisor: Petri Kirves M.Sc. (Tech.)

Radio telescope is an astronomical instrument and an essential tool of radio astronomy. It is consists of a radio receiver and antenna system. The design of antenna system of the radio telescope is a critical issue because of the demand of wide bandwidth, high gain, directional beam, and circular polarization. Metsähovi radio observatory has proposed a project named Metsähovi compact array to build four radio telescopes in order to create new research platform in different areas, such as radio astronomy, solar research, and space physics. In this master thesis work, a wide band feed for the reflector antenna of the proposed radio telescope is analyzed and designed. Initially several solutions are studied and analyzed. Based on these studies, a two arm conical log spiral antenna (CLSA) is designed and constructed in CST. At first, a theoretical model of CLSA is developed. Further, the design equations are reformulated to simulate the model in CST. The simulation results shows good agreement with the theoretical model. Moreover, the antenna is also simulated with the bifilar lines to have an practical feeding system of the antenna. In this case the results shows poor performance due to the significant radiation coming out from the bifilar lines which is overlapping with the antenna radiation. To avoid this radiation, a hollow metal is introduced which covers the bifilar lines to block the radiation coming out from the bifilar lines. The antenna performance with bifilar lines satisfies most of the requirements that has set up for this work. Besides, a mechanical construction of the antenna is presented to protect the antenna from the outside environment.

Keywords: CLSA, circular polarization, gain, HPBW, input impedance, reflector antennas, return loss, radiation pattern, wide band

Preface

First of all, thanks should be forwarded to Almighty ALLAH, most gracious, most Merci-full, who guides me in every step I take. This master thesis is based on research work conducted at the department of Electronics and Nanoengineering in collaboration with Metsähovi Radio Observatory (MRO).

I would like to take this opportunity to express heartfelt gratitude to my supervisor Prof. Anne Lähteenmäki for giving me the opportunity to execute this thesis. I would like to thank her for her advice, guidance, and valuable suggestions regarding my thesis. I would also like to thank my instructor Petri Kirves for his instructions and coaching. His wide knowledge in the research field in both theory and practice, created a very valuable work experience for me.

I would like to thank Dr. Jari Holopainen and Md mazidul Islam for their comments and constructive suggestions regarding the antenna design and simulation. I also want to thank F. M. Mahafugur Rahman for his comments, suggestions, and corrections in scientific writing.

I would like to express my deepest gratitude to my uncle Dr. Mohammad Abdul Jabbar ,who has always been by my side and provided me with unwavering support throughout my life.

Finally, I would like to thank my family, especially my parents for providing continuous guidance and wholehearted support throughout my life.

Espoo, 23.01.2017

A K M Monsurul Alam

Contents

Symbols and abbreviations

Symbols

α	Conical angle
θ_0	Wrap angle
δ	Angular width of the arm
D	Lower cone diameter
f_u	Upper frequency
f_L	Lower frequency
H	Height of the cone
L	Length of the spiral
d	Upper cone diameter
r_u	Upper radius of the cone
r_L	Lower radius of the cone
r	Radius of the bifilar Line
ρ_o	Initial radial distance
Z_o	Characteristics impedance

Abbreviations

CST	Computer Simulation Technology, an electromagnetic simulation software
CLSA	Conical log spiral antenna
HPBW	Half power beam width
MCA	Metsahovi compact array
MRO	Metsahovi Radio Observatory
UWB	Ultra wide band

1 Introduction

Radio astronomy plays a vital role in modern-day astrophysics and is a key complement to optical astronomy. Radio astronomy is the discipline of astronomy whose study technique is based on the capture and analysis of radio frequency electromagnetic radiation using radio telescopes, the major tool of radio astronomy [1].

Radio telescopes are used to study naturally occurring radio emission from stars, galaxies, black holes, and other astronomical objects. It is also used to transmit and reflect radio light from planetary bodies in our solar system. A radio telescope system consists of various different parts, and among them the antenna system is an important one. Large parabolic reflector antennas are often used in radio telescopes and designing the feed of the reflector antennas has always been a challenging task as many factors, such as wide bandwidth, input impedance, high constant gain over wide frequency range, beam width, and polarization need to be considered while designing the feed [2].

Metsähovi Radio Observatory (MRO) is a separate institute of the Aalto University school of electrical engineering and the only radio astronomical observatory in Finland. It has received four 5.5-metre bare-bone dish as a donation. They will work as a radio telescope for study and research purpose in Metsähovi Radio Observatory. In order to put them in to operation they need to be equipped with receivers, steering, and recording systems. Furthermore, they will become a radio interferometer after connecting together with correlate system in order to obtain better resolution and sensitivity compared to single telescope. To achieve those goals, equipping, installing antennas, and transformation of existing system is required so that a complete working telescope system can be put in to operation. For this purpose, a project named Metsähovi compact array (MCA) has been proposed [3].

The objective of the proposed Metsähovi Compact Array (MCA) is to build the first radio interferometer in Nordic countries. It will create a new research platform in different areas, for example, radio astronomy, solar research, and space physics. It will also be significant for Metsähovi Radio Observatory to ensure the participation in high profile international collaborations. Moreover, it will play an important role

in hands-on learning in different disciplines, and students in radio astronomy and radio science will get an opportunity to involve themselves in building and in the operation phase of the interferometer [3].

The goal of this master thesis work is to design a wide band feed for a reflector antenna, which will be a candidate for a radio telescope of the proposed Metsähovi compact array (MCA). There are some specifications which have been set up for this this work:

- Frequency range 5 GHz to 15 GHz
- Dual circular polarizations
- High constant gain over wide frequency range
- Beam width (-10 dB level) 120° to 150°
- Rugged construction

In this study, a two arm conical log spiral antenna (CLSA) is investigated based on the requirements of the the MCA project. Initially various classes of wide band antennas are studied and after the analysis, CLSA is designed and examined. The designed CLSA falls under frequency independent antennas. It is found that this kind of a frequency independent antenna is most suitable for the MCA project because of its uniform performance characteristics, for instance, input impedance, beam width, gain, and circular polarization over a wide range of frequencies.

During the 1950s, the idea of conical spiral antenna was first presented by Rumsey [4, 5]. Two compulsory orders were introduced for practical frequency independent antennas: the angle principle and the truncation principle. The angle principle states that the antenna performance is completely described by angle, and hence the geometry of the antenna will be infinite and the antenna will be frequency independent. In truncation principles, an active region of a finite size antenna is considered. The active region is define as the part which is responsible for most of the radiation in one frequency and it moves on the antenna with the change of frequency so that the dimension of the region, which is expressed in terms of wavelength, remain constant. As a result, the antenna is practically frequency independent over a wide range of frequencies when the active region moves on the finite structure of the antenna.

The equiangular spiral antenna is a class of frequency independent antennas which is defined entirely by angles. It was first established by Dyson [6–8]. He experimented on these kind of antennas and developed design curves to present antenna characteristics in terms of HPBW, directivity, and axial ratio. His experiment involves the measurement of current distribution on the arms of CLSA. He found that the current is minimum at the outside of a region at a particular frequency in which most of radiation accrues. As a result, most of radiation in that particular frequency is created by that region. He defined this region as an active region.

A two arms conical spiral antenna based on thin metal and expanded arms for submarine communications was studied by Wills [9]. The conical spiral antenna with expanding arms was also experimented by Ramsdale [10]. He introduced a technique to enhance the performance of the antenna at low frequencies. His method involves a termination of the big end of the spiral by lumped resistors for impedance matching at lower frequencies. The goal of the matching is to reduce the reflection at that end because high reflection is responsible for performance degradation at lower frequencies. His experiment proves that a remarkable improvement of impedance matching at low frequencies can be achieved using this technique.

The feeding of conical spiral antennas is always challenging as they are balanced structures because of their symmetry. On the other hand, coaxial cables that are normally used for feeding purposes are unbalanced. Therefore a balanced impedance transformer is required between them so that the impedance will match at both ends of the feeding ports. This impedance transformer is generally known as transformer type balun. Dyson implement the first balun for CLSA. This is known as an infinite balun [7].

In this Master's thesis work a conical log spiral antenna is designed and investigated based on Dysons experimental data, in order to fulfill the MCA project demands. To achieve the targets, various types of spiral antennas are studied and analyzed and based on this a theoretical model of CLSA is developed. This theoretical model is implemented and simulated in CST: Microwave studio [11]. Finally, the theoretical model and the simulation results are validated in terms of reflection coefficient, beam width, gain, and axial ratio.

This thesis is divided into six sections. In Section 2 a comparative study of wide band antennas concerning reflector feed are presented. The theoretical design procedures of CLSA are described briefly in Section 3. Discussed about the simulation process of CLSA in CST is presented in Section 4. Also the results of the simulation in terms of return loss, input impedance, beam width, gain and axial ration are presented in this section. In Section 5 the different types of feeding techniques of CLSA are explored. Finally Section 6 provides a summery of this work and further guidelines for the future works are given.

2 Study of Wide band Antennas

This chapter gives an overview of wide band antennas and its fundamental properties, focusing on its use in reflector antenna as a feed. At the beginning, important antenna parameters regarding wide band antennas are discussed. Moreover, different kind of wide band antennas and their merits and demerit's are disputed.

2.1 Wide band antenna properties

There are some essential antenna parameters need to be studied for designing broadband antennas for instance, radiation pattern, gain, directivity, impedance matching, and radiation efficiency. Its required to have more less constant value of them in wide band antennas [12]. But those parameters can vary in different frequencies and that's make the design of wide band antenna challenging. Some vital antenna parameters are described below.

2.1.1 Return Loss

The return loss describes the amount of power that is transferred by the antenna. Due to impedance mismatch between transmission line and load, a portion of incidence signal reflected back toward the generator. The return loss is define as the ratio of incident power to the power reflected back from the antenna. Mathematically is can be represent as:

$$RL = 10 \log_{10} \frac{P_{in}}{P_{ref}} \tag{2.1}$$

Where P_{in} is incident power and P_{ref} is reflected power from the antenna. The ratio of P_{in} and P_{ref} should be high in order to get maximum power transfer. Generally 10 dB return loss considered a good one as it means almost 90 percent of the input power is radiated by the antenna if we consider there is no ohmic losses.

2.1.2 Input Impedance

The ratio of the voltage to current at the input terminal is define as the input impedance of the antenna. Figure 2.1 shows a circuit model of the antenna where antenna is represented with impedance Z_{A} and input impedance of the antenna is represented by Z_{in}.

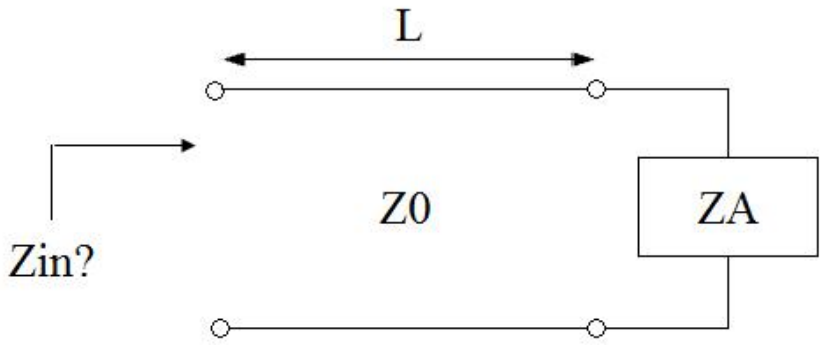

Figure 2.1: Circuit model of an antenna

.

The input impedance of the antenna is mostly depended on the characteristics impedance of feeding transmission line of the antenna if the transmission line is separated form the antenna. [13]. Also its largely effected by the line width, distance between the lines, dielectric constant and thickness of the substract [14] [15] [16].

2.1.3 Radiation Pattern

The graphical representation or a mathematical function of the radiation properties as a function of a space coordinate is defined by the radiation pattern. The properties of the radiation patterns are radiation density, radiation intensity, field strength, directivity, and polarization. Radiation pattern has many parts such as main lobe, side lobes, and back lobes. The radiation lobe is a portion of a radiation pattern regions bounded by relatively week radiation intensity.

A three dimensional polar pattern with number of lobes is shown in figure 2.2(a). The lobe that contain maximum radiation is called main lobe. Any lobe excecpt the major lobe is side lobe and the lobe that is opposite to the main lobe is called back lobe. In other worlds, the back lobe is pointed at 180° from the main lobe. In 2.2(b) the major lobe is pointing at $\theta = 0$.

Depending on the direction of the main beam, the radiation pattern can be classified into isotropic ,directional and omni-directional radiation pattern. Isotropic radiation means the antenna having equal radiation in all direction. The isotropic antenna is exists only in theory. When the radiation of the antenna goes more effectively in

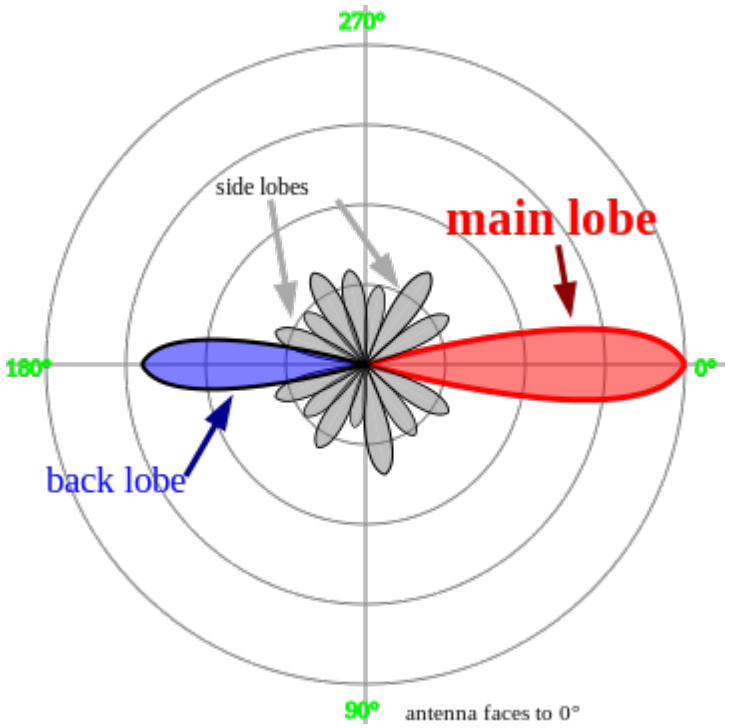

(a)

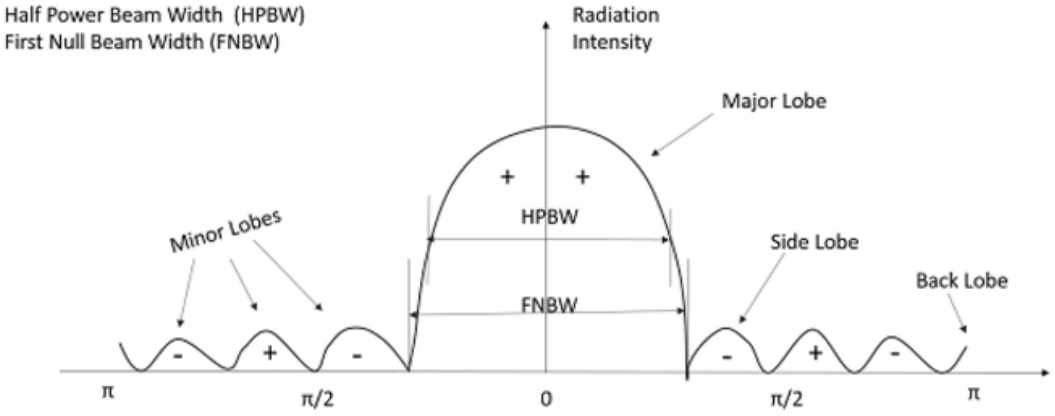

(b)

Figure 2.2: (a) Radiation lobes of the antenna; (b) Linear plots of the power pattern [17].

some direction its called directional radiation pattern. The omni-directional radiation means the radiated wave is distributed uniformly in all direction in one plane. This radiation pattern is often described as "doughnut shaped". Omni-direction radiation pattern is different from isotropic radiation which radiates equal power in all directions and has a "spherical" radiation pattern.

2.1.4 Radiation Intensity

Radiation intensity is a far-field parameter of an antenna. Its defines as the power radiated from an antenna per unit solid angle. It can be represent mathematically as follows:

$$U = r^2 W_{rad} \tag{2.2}$$

Where U is radiation intensity and is W_{rad} radiation density.

2.1.5 Gain, Directivity and Radiation Efficiency

Directivity is a measure of how much intensely the antenna is radiating in a preferred direction. It is an important parameter of an antenna. It can be define as the ratio of radiation intensity to the average radiation intensity over all direction. The average radiation intensity is equal to the total radiated power divided by 4π. Thus it can be calculated by:

$$D = \frac{4\pi U}{P_{rad}} \tag{2.3}$$

Another vital parameter of the antenna is gain which is closely related to the directivity. It is the measure of antenna ability to concentrate radio waves in a particular direction. Gain can be represent similarly the way directivity is represented mathematically, only difference is while calculating the gain , radiation efficiency is taken into account. So the gain can be written as:

$$G = e_{rad} D \tag{2.4}$$

Where G is the gain and e_{rad} is the radiation efficiency of an antenna. The ratio of the radiated power to the input power at the terminal of the antenna is called radiation efficiency. It can be written as follows:

$$e_{rad} = \frac{P_{rad}}{P_{in}} \tag{2.5}$$

Where P_{in} is the input power at the terminal of the antenna.

2.1.6 Beam Width

Beam width is one of the crucial parameter of an antenna specially when antenna is to be designed as reflector feed. The beam width is classified commonly is two types. They are half power beam width (HPBW) and first null beam width (FNBW). IEEE

defines the HPBW as: "In a plane containing the direction of the maximum of a beam, the angle between the two directions in which the radiation intensity is one-half value of the beam." It is also known as beam width at -3 dB level. FNBW is defined as the angular separation between nulls of the main beam. Figure 2.3 showing two dimensional field and radiation pattern where HPBW and FNBW are explained graphically.

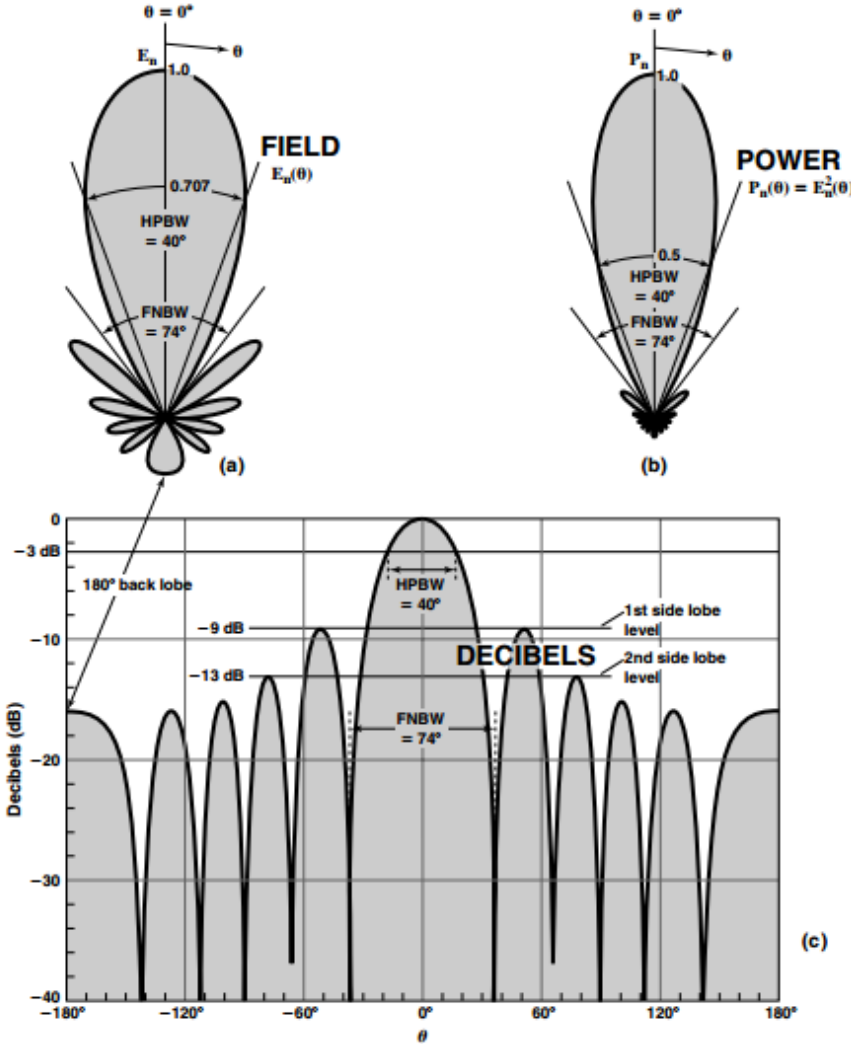

Figure 2.3: Two dimensional field and power radiation pattern [17]

.

In addition to HPBW and FNBW, the antenna can be designed to get the desired beam width at different level such as at -6 dB , -9 dB , -10 dB etc. In order to get sharp beam or in other words high gain, the side lobes level should be low. There is a trade off between the main beam and side lobes. When the main beam gets sharp the side lobe level goes up. This phenomena is often observed at -3 dB and -6 dB level beam width. But it is seen that at -10 dB or -12 dB level, we can get broader beam as well as low level of side lobes. This is why some application demands beam

width at -10 dB or -12 dB level.

2.1.7 Bandwidth

One of the main characteristics of the broadband antenna is its bandwidth. Bandwidth define as the range of frequencies at which the antenna shows its desired characteristics. Bandwidth of the antenna can be describe mathematically using higher, lower, and centre frequency of the antenna. It can be written as:

$$BW = \frac{f_H - f_L}{f_c} * 100 = 2\frac{f_H - f_L}{f_H + f_L} * 100 \tag{2.6}$$

Where f_{H} is the highest frequency, f_{L} is the lowest frequency and f_{c} is the center frequency of the band. The center frequency can be calculated from:

$$f_c = \frac{f_H + f_L}{2} \tag{2.7}$$

Bandwidth also can be represented in terms of ratio to highest and lowest frequency for broadband antennas. It is given by:

$$BW_{\mathrm{wideband}} = \frac{f_H}{f_L} \tag{2.8}$$

2.1.8 Polarization

Polarization is one of the main characteristics of the antenna. Polarization simply define the orientation of the electric field vector. This electric field vector is perpendicular to both the direction of travel and the magnetic field. Polarization is most important parameter as its ensure maximum amount of signal reception at the receiving end. Polarization can be classified into linear, circular, and elliptical polarization.

Linear polarization means at a given point in space the electric field vector at that point is always oriented along the same straight line at every instant of time. This is happens when two orthogonal linear components are in phase or out of phase. Vertical and horizontal polarization are two category of linear polarization. In linear vertical polarization, the electric filed vector of the electromagnetic wave is perpendicular to the earth. This is achieved by placing the antenna vertical to the earth. On the other hand, when electric filed vector of electromagnetic wave is parallel to the earth it is called horizontal polarization and it can be achieved by placing the antenna horizontal to the earth. Figure 2.4 showing vertical and horizontal polarization with the direction of electric and magnetic field.

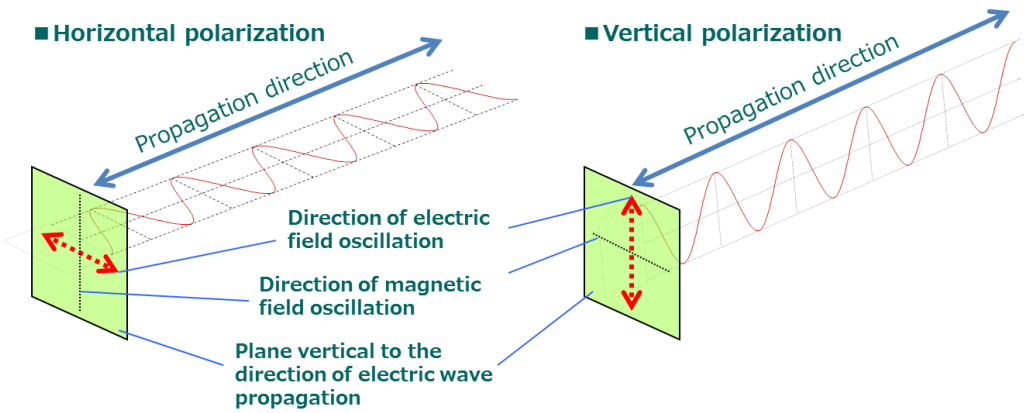

Figure 2.4: Vertical and horizontal linear polarization

.

In circular polarization the electric field vector traces a circle as a function of a time at given point in space. To get circular polarization following factors should be considered:

- The field must have two orthogonal components
- The two component must have same magnitude
- The two component must have a time phase deference of odd multiples of 90^0

Graphical representation of the circular polarization is shown in figure 2.5, where we can visualize the rotation of the electric field vector due the the phase difference of the two orthogonal components. There are two types of circular polarization. They are left hand circular polarization (LHCP) and right hand circular polarization (RHCP). When the rotating electric field vector rotates clockwise then its called RHCP and similarly anticlockwise rotation is known as LHCP. Circular polarization is most often use in satellite and space communication. Since linear polarization may be changed its polarization because the signal passes through many anomalies (such as Faraday rotation) in the ionosphere. In addition, the polarization of the signal also can be changed due the the position of the satellite or any object of the space respect to the earth station. This polarization change means the vertical polarized signal may changed into horizontal or vice verse. Since circular polarized wave can radiates or receive energy in both vertical and horizontal plane, this is desired for the space and satellite communication.

The elliptical polarization is similar to the circular polarization only difference is the rotation of the electric field vector is elliptical instead of circular. This is because the magnitude of the two orthogonal components may changes with time whereas in circular polarization the magnitude of the two orthogonal components is constant with the change of time. Figure 2.6 shows the elliptical polarization graphically.

In order to achieve elliptical polarization following factors should be considered:

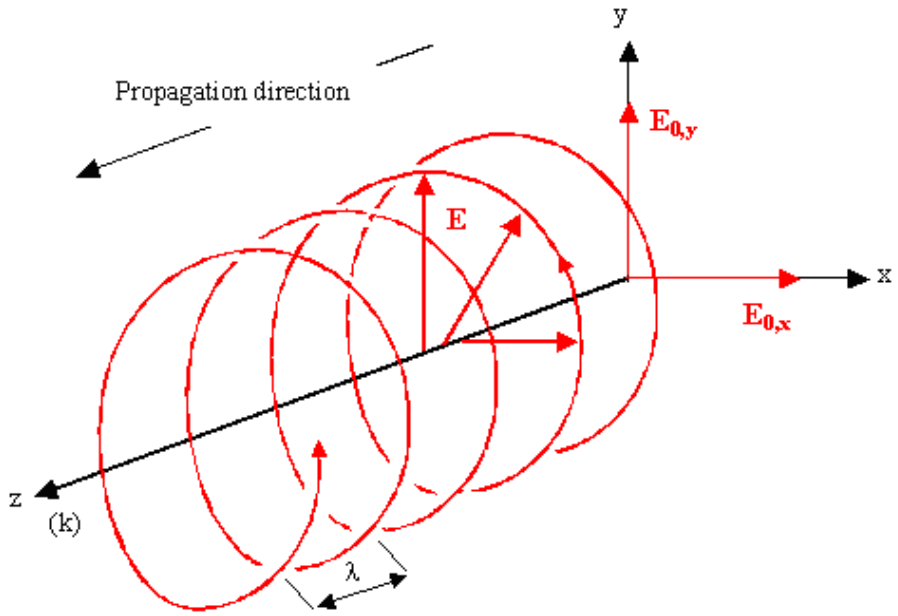

Figure 2.5: Circular polarized electromagnetic wave

.

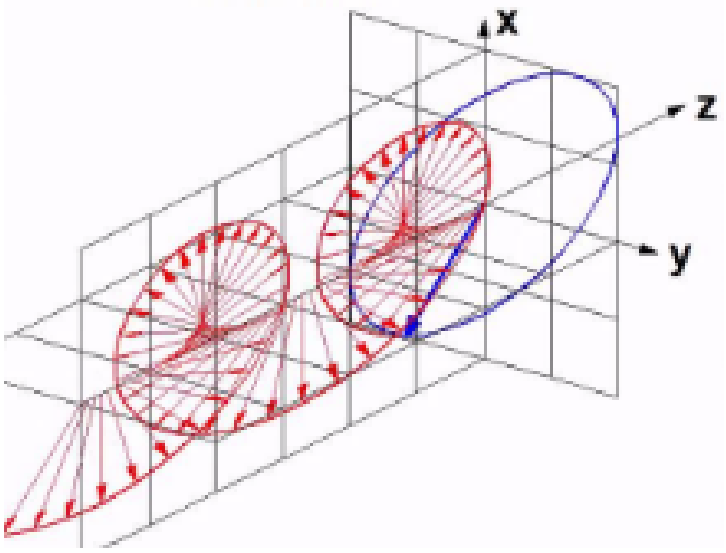

Figure 2.6: Elliptical polarized electromagnetic wave

.

- The field must have two orthogonal components
- The two components can be off the same or different magnitude
- If the two component are of the same magnitude, the time phase difference between the two components must not be 0° or multiples of 180°(Because it will be then linear)
- If the two component are of the same magnitude, the time phase difference

between the two components must not be odd multiples of 90°(Because it will be then circular)

2.2 Wideband Antennas

Wide band antennas are key thing in wireless communications. Demand of the wide band antennas are growing up due to its unique performances that's can meet all the requirements that are needed now a days. It is important to find out proper wide band antennas which suitable for the intended application. In this project, various kind of wide band antennas are examined and spiral antenna is chosen due to its simple structure, low profile, wide bandwidth, and circular polarization.

2.2.1 Frequency Independent Antennas

Frequency independent antennas are well known wide band antennas because of its constant radiation characteristics, impedance and circular polarization over large bandwidth [18] [19]. There are various types of frequency independent antenna such as sinuous, equiangular, and archimedean [20]. The design and optimization of the frequency independent antennas is simple because these antennas can completely defined by the angles. Mathematical representation of shape of the antenna is given in equation 2.9, which is taken from reference [4].

$$\rho = e^{\alpha(\phi+\phi_0)}F(\theta) \tag{2.9}$$

Where ρ, θ and ϕ are the spherical coordinates, α and ϕ_0 are constants and $F(\theta)$ is any function of θ.

The main advantages of the frequency independent antennas is its uniform behaviour over a wide frequency range. Moreover, the design and optimization of this kind of antenna is simple and easy. However, this kind of antenna has broad beam width and low gain which is not suitable for some applications. Many research has been done and techniques has been developed to overcome this issue. Those includes modification of the antenna, making array of frequency independent antennas and many more.

2.2.2 Log-Periodic Antenna

Log periodic antenna is a class of antenna which has wide band frequency characteristics and its introduces in reference [21]. The structure of the log periodic antenna progress logarithmically and hence the characteristics of the antenna changes periodically with the logarithm of the frequency. The design of log periodic antenna can be classified based on three concepts. First design concept is the geometry of the antenna can be defined using angles rather then length. Second principle is

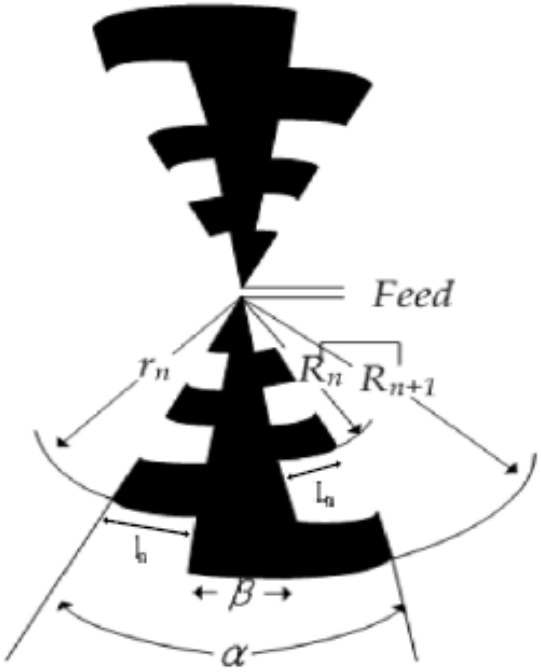

Figure 2.7: Geometry of the log periodic antenna [21]

.

the input impedance of the antenna in independent of the frequency. Hence it is also a frequency independent antenna. Third one is the electrical properties of the antenna repeats periodically with the logarithm of the frequency. This periodical repetition of electrical properties can be achieved from the logarithmic structure of the antenna.

Figure 2.7 shows the stucture of a log periodic antenna where R_{n} is the radii of the antenna, r_{n} is slot radii and β is subtended angle. The mathematical definition of the antenna is defined in following equation 2.10, where R_{n} , $R_{\mathrm{n-1}}$ and $R_{\mathrm{n+1}}$ form a geometric sequence term.

$$\tau = \frac{R_n}{R_{\mathrm{n+1}}} \tag{2.10}$$

Using R_{n} , $R_{\mathrm{n-1}}$ and $R_{\mathrm{n+1}}$, it is possible to derive same geometric ratio. The successive slots and distances are in common ratio, which is denoted by M.

$$M = \frac{r_n}{R_{\mathrm{n}}} = \frac{l_n}{L_{\mathrm{n}}} \tag{2.11}$$

An broad study on these kind of antennas is done in reference [22] as a function of

α, β, τ and M. In general, this type of antenna has planer and conical structure and they have linear polarization.

2.2.3 Spiral Antenna

Spiral antenna is well known wide band antenna and it has been using in many applications. It is also a class of frequency independent antenna. It can have wide range of frequency. Besides, other performances such as input impedance and radiation pattern of this antenna is constant over wide range of frequency. The design of the spiral antenna is very simple as it performance can be characterize using its angles. The lower and the higher frequency of the spiral antenna is determined by the higher and lower circumference of the antenna. In general the spiral antenna is made of wire consist of thin metal. Spiral antenna can also be printed on substract. Depending on the application, the spiral antenna is designed in different ways.

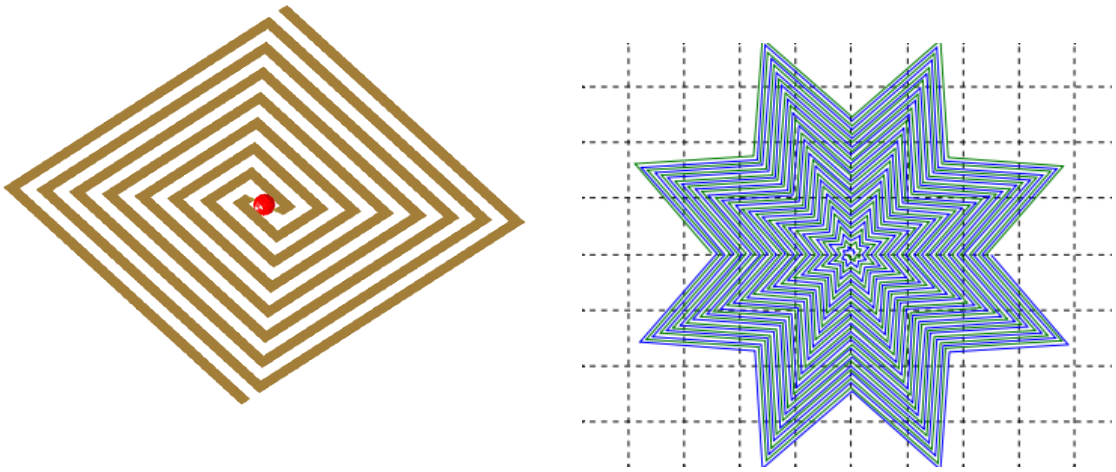

(a) (b)

Figure 2.8: (a) Squire Spiral; (b) Star Spiral

The spiral antenna is usually bi-directional which is a demerits for many cases as most of the application requires directional radiation pattern. Many research and techniques has been developed to get directional radiation pattern from spiral antenna. Among them one techniques is to add lossy cavity to the antenna backed by a conductor which improves the performance of the antenna at low frequencies. The back conductor works as a reflector and redirect the radiation which makes the radiation pattern unidirectional. The lossy cavity improves the low frequency behaviour and the axial ratio by reducing the current from the each end of the spiral arms. Furthermore, a ring shape absorbent material can be applied to cavity in order to reduce the reflection current to the each end of the arms of the archimedean spiral [23]. It provides a large pattern bandwidth since it absorbs the back radiation from the spiral which reduce the reflection coming from the ground plane that causes

patterns nulls [24]. However, this lossy cavity is responsible for gain reduction due to its losses. In addition, its gives extra depth and weight to the antenna. Without the back reflector the spiral antenna is bidirectional. In order to get directional radiation pattern back reflector has been using in many applications [25]. Another method to improves the spiral antenna performances is to add absorbing material. In absorbing material backed spiral antenna, the reflected wave from the cavity will be attenuated which gives wide band characteristics to the antenna. However, use of the absorbing material is not approved for some application due to the reduced gain.

(a) (b)

Figure 2.9: (a) Archimedean Spiral l; (b) Equiangular Spiral

Size of the spiral antenna is another important issue that has been considered for many years. In general, the size of these antennas is large compare to others. There are many formulas has been developed to reduce the size. One of the way to reduce the size is through material loading. But this gives loses and weight which can be a problem for some applications. To rid out of this problem size can be reduced using slow wave techniques. This slow wave is achieve by modifying the antenna structure with zigzag or sine shape which increase the circumference of the spiral. There are many other techniques that can reduce the size such as choosing small starting angle [26] and implementation of electromagnetic band gap (EBG) [21].

Spiral antenna has many classifications and they are classified according to their shape and structure. Some of the spiral antennas are square spiral, star spiral, archimedean spiral, and equiangular spiral. The performances of square and star spiral are better in low frequencies but square spiral is less frequency independent in high frequencies [27]. Size reduction of the star and squire spiral is almost same but star array allows tighter packing which squire spiral does not allows [28]. However, star and squire spiral has dispersive behaviour which is a great disadvantage. Archimedean spiral is the most widely used spiral antenna due to its large bandwidth and allowing tighter array spacing. Similarly equiangular spiral antenna

is also widely used in many applications which has similar characteristics to the archimedean spiral antenna.

2.2.4 Equiangular Spiral

Equiangular spiral antenna is one of the modified version of the spiral antenna. Its surface is described by angles and its performance is frequency independent. Figure 2.10 shows the geometry of equiangular spiral antenna. The total length of the antenna can be calculated using following equation:

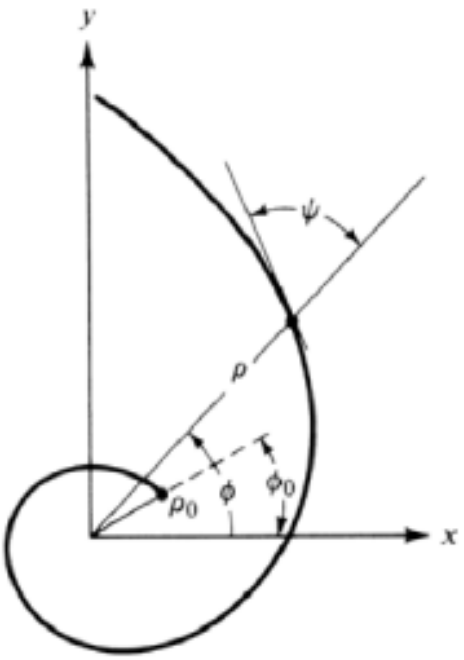

Figure 2.10: Geometry of the Equingular spiral antenna

.

$$L = \int_{\rho_0}^{\rho_1} [\rho^2 (\frac{d\phi}{d\rho})^2 + 1]^{\frac{1}{2}} d\rho = (\rho_1 - \rho_0)\sqrt{1 + \frac{1}{a^2}} \tag{2.12}$$

and

$$\rho = ke^{a\phi} \tag{2.13}$$

Where ρ and ϕ are polar coordinates and a and k are positive constant. Equingular spiral has many advantages. Because of its progressive structure it can provide constant performance over wide range of frequencies [6]. However, this type of antenna has large size which is not suitable for the applications where compact size is required.

2.2.5 Archimedean Spiral

Archimeadean spiral antennas is one the popular antenna among the spiral antennas and it has been used in various kind of application such as satellite communication, UWB communications, radio navigation's, and radar [16]. This antenna was developed by E.M. Turner [28]. The most benefits of this antenna are simple design and easy to fabricate using printed circuit technology. It is not truly frequency independent antenna because the spacing between the adjacent arms is specified by a constant not angles. Hence it can not provide very large bandwidth. It is also called quasi frequency independent antenna [29].

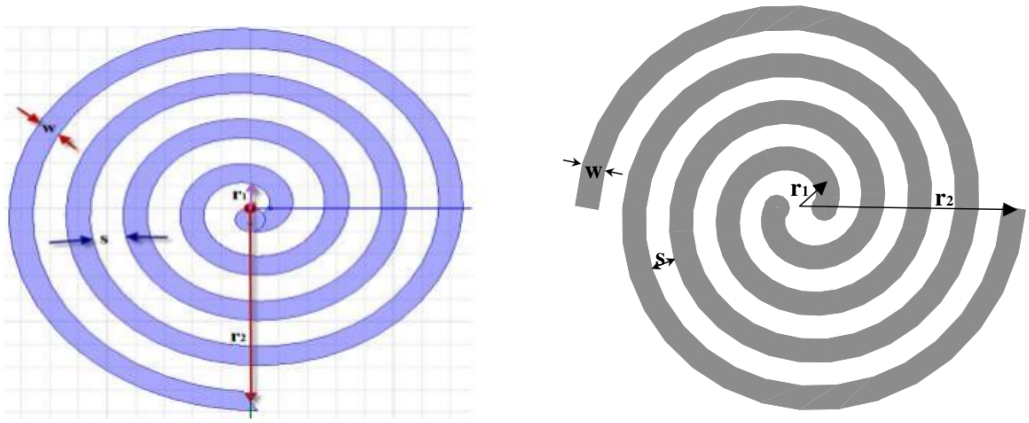

(a) (b)

Figure 2.11: (a) Single Arm Archimedean Spiral ; (b) Two Arm Archimedean Spiral

This antenna has many advantages such as low profile, low weight, high efficiency, circular polarization, stable impedance characteristics, and wide bandwidth. Because of these advantages, it is widely used in many applications. The archimeadean spiral is classified by number of arms. There are three types of archimedean spiral. They are single arm, double arm, and four arm archimedean spiral. The design procedure of the dual arm is similar to the single arm. Only difference is that, the dual arm is obtained by placing a duplicate arm with 180° rotation. The arms of the archimedean spiral is linearly proportional to the winding angle ϕ and using this the governing equation of the archimedean spiral can be written as:

$$r = r_0\phi + r_1 \tag{2.14}$$

and

$$r = r_0(\phi - \pi) + r_1 \tag{2.15}$$

Where r_1 inner radius and r_2 outer radius. The mathematical equation for calculating the lower cutoff frequency which is depends on outer radius r_2 is as follows [18]:

$$f_L = \frac{c_0}{2\pi r_2 \sqrt{\epsilon_{eff}}} \tag{2.16}$$

The inner radius of the achimedean spiral determines the higher cut off frequency, which is as follows:

$$f_H = \frac{c_0}{2\pi r_1 \sqrt{\epsilon_{eff}}} \tag{2.17}$$

2.2.6 Array of Wideband Antennas

Wide band antennas typically have broad radiation pattern and low gain which is a major disadvantage as some application requires directional radiation pattern and high gain. Besides that, some applications such as communications services, navigation systems, and broadcasting systems demands multiple antennas. This problem can be overcome by forming array of wide band antennas. Wide band array has some significant advances over single wideband antenna. Some benefits are sharp gain, directional beam, and more control over radiation pattern which allows to steer the beam to the desired directions. However, forming an array can destroy the antenna performances if the spacing between two adjacent antenna is not specified properly. Inter-element spacing is very important for designing an array because it can effect the size of the antenna and also can increase the mutual coupling effect.

Larger inter element spacing provides less mutual coupling effects but gives less space to pack more elements. In addition, large inter element space forms grating lobes which is not desirable. At high frequency of operation, the inter element spacing needs to be increase in order to avoid the mutual coupling effects which allows the formation of grating lobes. Formation of the grating lobes responsible for the limiting the array bandwidth and its not desirable. The effects of different unequal spacing such as logarithmic spacing and non-monotonically spacing is investigated in reference [30]. It is found from the investigation that, unequal spacing gives more space to pack more element with preferred bandwidth compare to the equal spacing. The theoretical models for analysing unequal or random spacing is developed by reference [31] and [32].

3 Conical Log Spiral Antenna

In this chapter theoretical design procedures of two arm conical log spiral antenna are described broadly. At first, the geometry and mathematical expressions of conical log spiral antenna are presented. After that, the parametric study of CLSA and its influence on CLSA characteristics are discussed. Finally based on Dyson parametric study and experiment, selection process of the CLSA parameters with regard of the MCA project requirements is presented.

3.1 Description of the CLSA

Frequency independent antennas are able to retain constant performance over a wide decade frequency range [33]. Spiral antennas are belongs to the class of frequency independent antennas due to their large bandwidth characteristic. There are many types of spiral antennas, such as helical, archimedean, pyramid, hemi spare or parabolic. Their performance characteristics are different from each other because of their dissimilar shape. They can be beneficial for many applications depending on their shape and size [25].

Conical log spiral antenna is a type of spiral antenna. It has some useful features, such as massive band width, circular polarization, and directional radiation pattern. This this kind of conical log spiral antenna was experimented by Dyson. He did his experiment by placing a log spiral on a conical structure for reducing the backward radiation associated with the planar equiangular spiral [35]. His study provides useful experimental data which makes the design of conical log spiral antenna easy and convenient.

The geometry of the conical log spiral antenna is shown in figure 3.1. The antenna is formed by winding a metallic strips around the surface of a truncated cone. The geometry of the CLSA can be define by three angles. They are half angle of the cone θ_0, the wrap angle α, and the angular width of the arms δ. The CLSA becomes a planar spiral when half angel θ =90° and its radiation pattern is bidirectional. The angle α defines the rate of warp of the arms around the conical surface. It is also

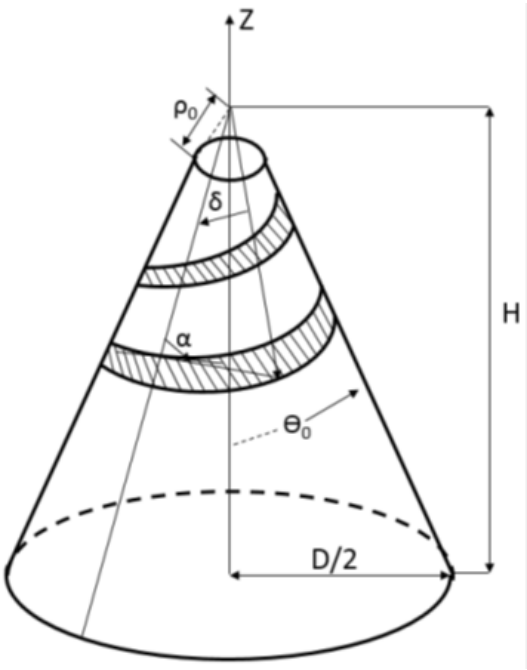

Figure 3.1: Geometry of two arm conical log spiral (CLSA) [34].

angle between the spiral arm and the radial line from the apex of the cone. The angle δ defines the constant angular width of the arms everywhere along the cone. In this study, the conventional design procedure is followed. One of the conventional way is to choose δ =90° and it is a most common configuration. It's also known as self-complimentary design and generally desired radiation pattern can be achieved using this configuration. The two arm conical spiral is constructed by placing the arms 180° apart form each other. In that case, the feed of the arms is balanced or in other words, arms are 180° out of phase with each other.

3.2 Governing Equations of CLSA

The conical log spiral is also known as the modification of equiangular spiral. It can be represent mathematically and the equation must be projected into three dimensions. Using the equiangular equation, the conical log spiral can be express as the radial distance, which is a function of the angle ϕ. Based on this relation, it can be written as:

$$\rho(\phi) = \rho_0 e^{\beta\phi} \tag{3.1}$$

Where β is defines as:

$$\beta = \frac{\sin(\theta_0)}{\tan(\alpha)} \tag{3.2}$$

In above equation, θ_0 and α are conical and wrap angle respectively. From the governing equation it is seen that, the radial distance is increases with ϕ that lies on any points on the spiral arm and it traces out the equiangular spiral on the conical face. Based on this, the initial radial distance from the apex of the cone ρ_0 can be expressed as:

$$\rho_0 = \frac{r_u}{\sin(\theta_0)} \tag{3.3}$$

The radial distance ρ_0 is an important parameter as its determines the upper radius r_u of the CLSA and the radiation pattern is greatly influenced by the upper radius. On the other hand, bottom radius of CLSA can be found out by the spiral arms at $\phi_{\max}$ angle and it does not affect the radiation pattern significantly. The lower and the higher frequency are determined by the lower and the upper radius of the CLSA respectively. Other useful parameter of CLSA can be found using simple geometry which are very handy for designing the CLSA. The height of the cone which measured from the apex of the cone to big end can be written as:

$$H = \frac{D}{2\tan(\theta_0)} \tag{3.4}$$

The height of the cone measured from the small end to big end can be written as:

$$H = \frac{D-d}{2\tan(\theta_0)} \tag{3.5}$$

And the total length of the spiral arms can be expressed as:

$$L = \frac{D-d}{2\cos(\alpha)\sin(\theta_0)} \tag{3.6}$$

If the CLSA is designed properly, the maximum radiation direction would go towards –z axis and in this direction the electric field is mostly circular polarized. Two types of circular polarization can be achieved from CLSA. They are left hand and right hand circular polarization. Both left hand and right hand circular polarization can be determined by the direction in which, the arms are wound around the cone. Figure 3.2(a) and Figure 3.2(b) shows the left hand and right hand circular polarized CLSA respectively.

3.3 The Active Region

It is important to study wave behavior and propagation along the spiral arms to understand the theoretical design of CLSA. For that, we have to know the definition of active region of CLSA. One of the interesting manner of CLSA is that, there

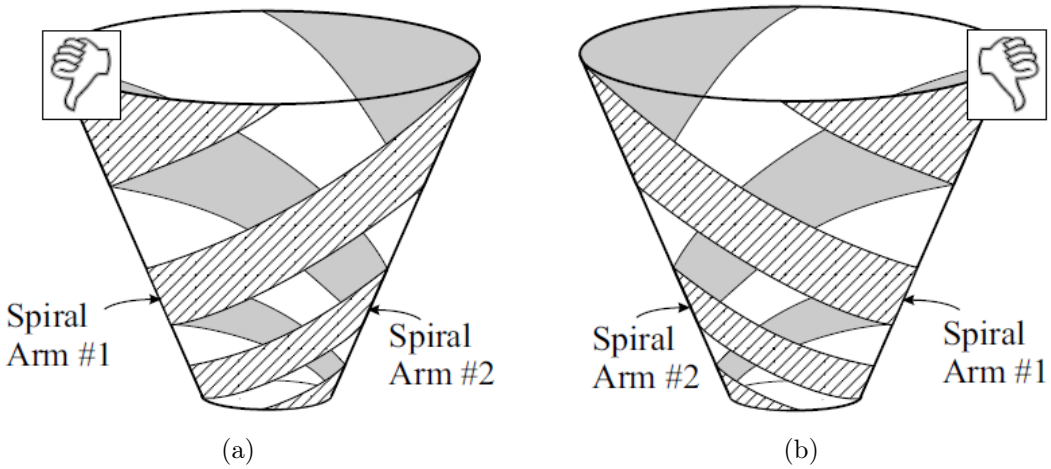

Figure 3.2: Diagram of the: (a) Left handed CLSA; (b) Right handed CLSA [36].

are certain parts of the antenna, which radiates most of the energy while other parts contribution is not significant. The region which is responsible for most of the radiation is called active region. The parts of antenna which are outside of the active region is in a slow wave configuration. In that region, the direction of the wave changes towards the vertex of the cone. As the frequency is increases the propagation constant is also increases and hence the slow wave configuration changes to fast wave configuration inside the active region. The tightly bound waves that are responsible for making slow wave has strong coupling with space travelling wave toward vertex of the cone. As a results, the propagation constant becomes complex [35]. Reduction in antenna size can be achieve by defining the active region of the antenna across the frequency bandwidth. Dyson illustrate a curve based on near field measurement to point out the area of active region which is shown in figure 3.3.

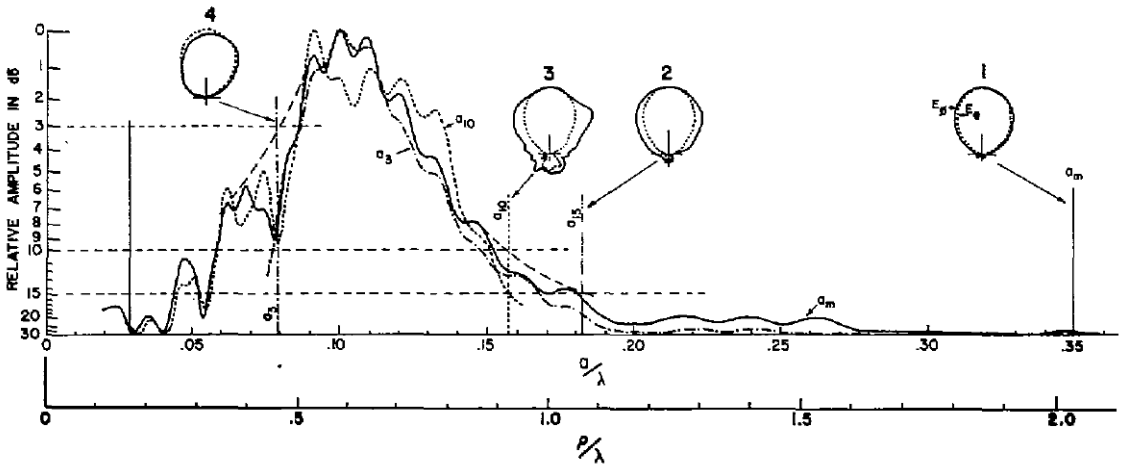

Figure 3.3: Electric far field radiation pattern corresponding to a truncation at indicated points (2θ=20°,α=80°, $\delta = 90^0$) [35].

In this figure, solid curves indicates the near field amplitude in dB and the numbers represent the radiation pattern. It is found in Dyson study that, there is an imperceptible change in radiation pattern with removal of turns from base end until the amplitude of the near field goes below 15 dBi. Because of this consequence it can be said that, it is possible to reduce the lower end side of the antenna with the sacrifice of negligible change in radiation pattern. This point could be identified as lower edge of active region which is denoted as $a_{15}{}^{+}$ in the figure 3.3. But radiation pattern starts to change significantly with further elimination of the turns. This further truncation in active region until the near field amplitude is 10 dBi, which is denoted by $a_{10}{}^{+}$. It has great impact on radiation pattern in respect of HPBW and axial ratio. Therefore, it's realizable to generalized lower part of the active region which can be represent as $a_{15}{}^{+}$ and $a_{10}{}^{+}$ for the near field reduction of 15 dBi and 10 dBi respectively. On the other hand, we can also represent the upper active region similarly, which has most influence in radiation pattern. In this case, the region is leveled as $a_{3}{}^{+}$, which is 3 dBi down from the maximum radiation. The truncation of the antenna below 3 dBi region will results major degradation in radiation pattern. It is possible to find the lower and the higher frequency of designed bandwidth using lower edge and upper edge of the active region respectively. Because the lower frequency band is depends on the lower cone radius and higher frequency is depends on the upper cone radius.

3.4 CLSA Parameters Analysis Inside the Active Region

It is clearly understood from the previous section that, locating the active region is crucial for designing CLSA. This active region must be realized for the antenna parameters, such as warp angle, conical angle, and operation bandwidth. Furthermore, finding proper radius of the cone in terms of wavelength is also vital. One of the key aspect of designing reflector feed is to guide the beam width. Antenna that is going to be used as a reflector feed should be designed in a such way that, the beam width can be generated according to the requirements. In this regards, active region plays a major role as it's directly related to the beam width. Now question is how to steer the far field radiation pattern by manipulating antenna parameter in respect of warp angle and conical angle.

From Dyson experiment, we can find the relation between conical and spiral angle concerning the beam width. The best way to understand the beam width is to represent it in terms of HPBW. In figure 3.4, we can see that, the upper and lower radius which is represented in terms of wavelength, are depends on both conical and spiral angle. We can also notice that, the directivity is depends on the spiral angle. It increases with the increase of the spiral angle. As a consequence, the HPBW will decrease because the directivity is a reciprocal function of HPBW . The principle behind this phenomena is that, the higher spiral angle means the greater turns and hence large active region. This leads to more number of element can be phased together for radiating energy, which can be realized in the figure 3.5, where

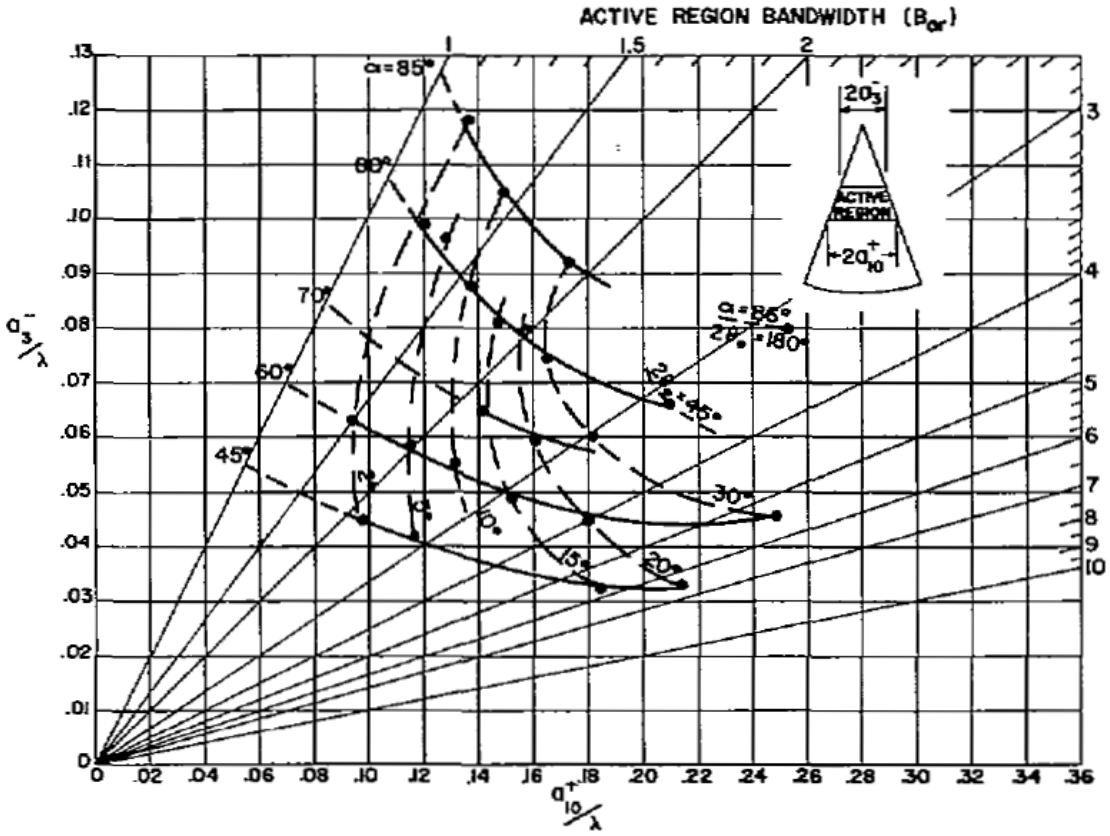

Figure 3.4: Active region constants with respect to wavelength of the CLSA [35]

the typical electric field radiation pattern is showed. At $\alpha = 80^0$ the generated beam is narrow as all the turns of active region is phased together. This principle can be understood from the figure 3.6, which shows the relative amplitude and the phase of magnetic fields measured along the surface of conical antennas and corresponding far-field radiation patterns . It can be seen that, at high spiral angle that means arms are would tightly, the radiated energy is more directive.

On the other hand less spiral angle results broader radiation pattern. Also increasing the spiral angle has the consequence of increase in the upper radius and decrease in the lower radius because of the shifting of active region. But this relation is valid above the warp angle 70°. Below this angle the relation is vice versa. Which means upper cone radius decreases and lower cone radius increases. The structure of the spiral becomes planar when conical angle goes towards 90°. The conical angle also has good influence on HPBW as the large angles provides wider active region which results broader beam.

When we are talking about HPBW, then we must need to discuss about the directivity. In chapter 2 we came to know that, directivity is a function of HPBW. It defines the concentration and direction of the radiated energy with the respect of antenna. The relationship between directivity and antenna parameters concerning

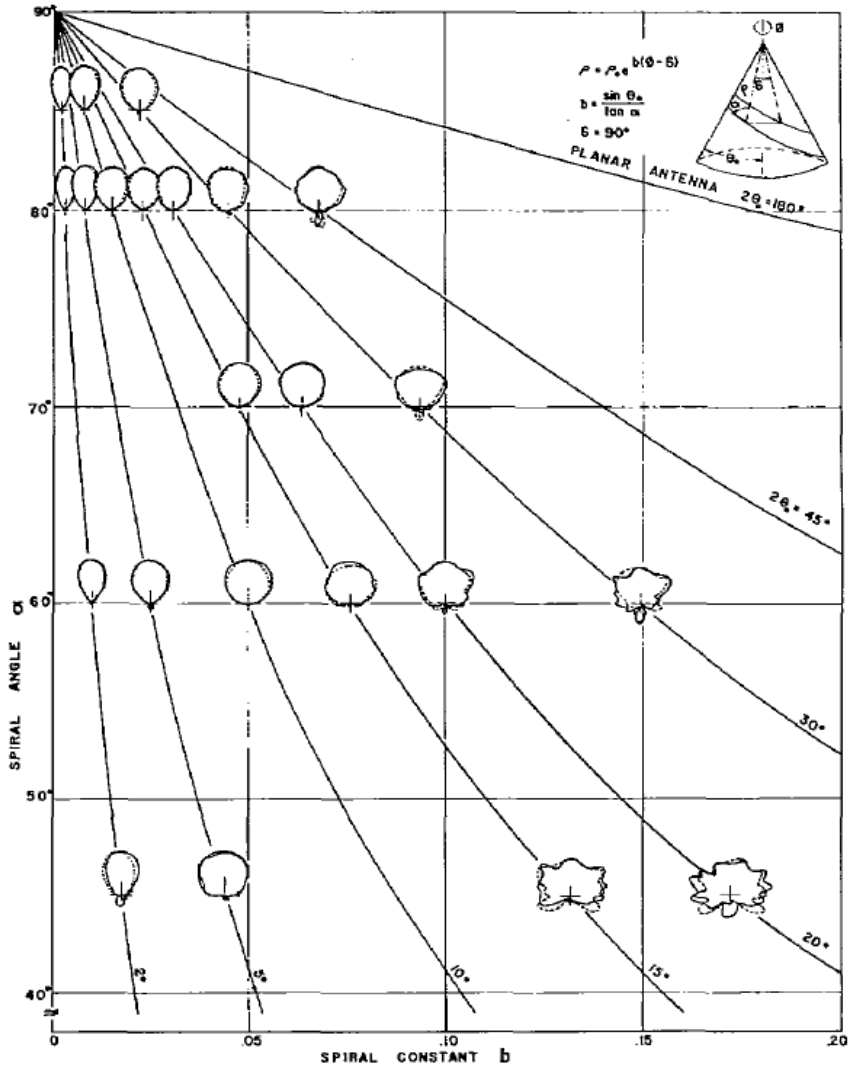

Figure 3.5: Typical electrci field radiation pattern for two orthogonal polarizations at δ=90° [35]

conical and spiral angle are described in the figure 3.7. Which indicates, the directivity gets high when spiral angle is increases. On the other hand, decrease in conical angle gives low directivity. Figure 3.7 is an important curve for designing CLSA because we can select our desired HPBW and directivity by choosing corresponding value of both conical and spiral angles and using them other parameters of CLSA can be found out.

Now to design the CLSA, proper value of both spiral and conical angle need to be chosen according to the demands of the application. For the MCA project, the required HPBW is in between 80° and 100° and the directivity value is $<$ 7 dBi. Considering above requirements, the spiral and conical angle selected as α=80° and θ_0=10° respectively from the figure 3.7. Based on this values, the upper and the

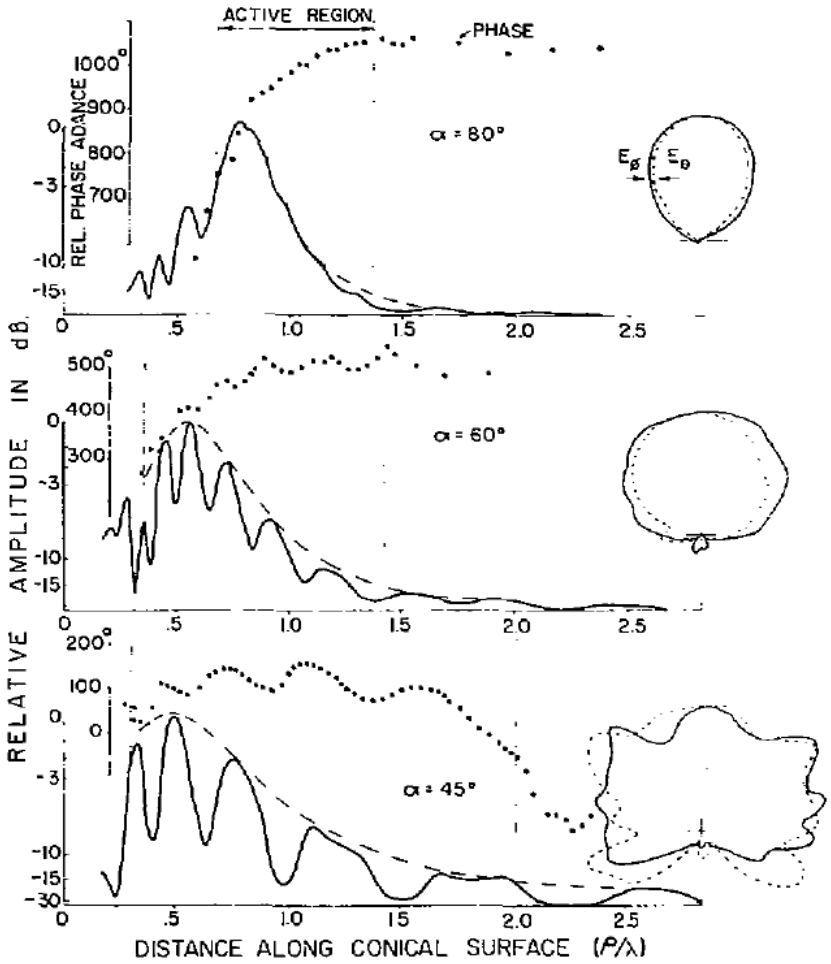

Figure 3.6: Relative amplitude and phase of magnetic fields measured along the surface of conical antennas and corresponding far-field radiation patterns [35]

lower radius can be found out from figure 3.5. With this parameters, the antenna performances are simulated using CST, which is described in chapter 4.

Another important feature of the spiral antenna is axial ratio. It defines the polarization state of the waves that are radiating form the antenna. The details definition of axial ratio is discussed in chapter 2. The axial ratio is also directly relevant to the active region. The target is to get as minimum axial ratio at the point where the maximum radiation occurs. It's possible to get smaller axial ratio at maximum radiation by increasing the spiral angel, as the increment of spiral angle provides less HPBW and high directivity. Figure 3.8 shows the correlation between axial ratio and spiral angle in terms of directivity. It can be seen that α =80° gives smaller axial ratio compare to α =70°. This is because at α =80° the half power beam width reduces which gives higher directivity and smaller axial ratio.

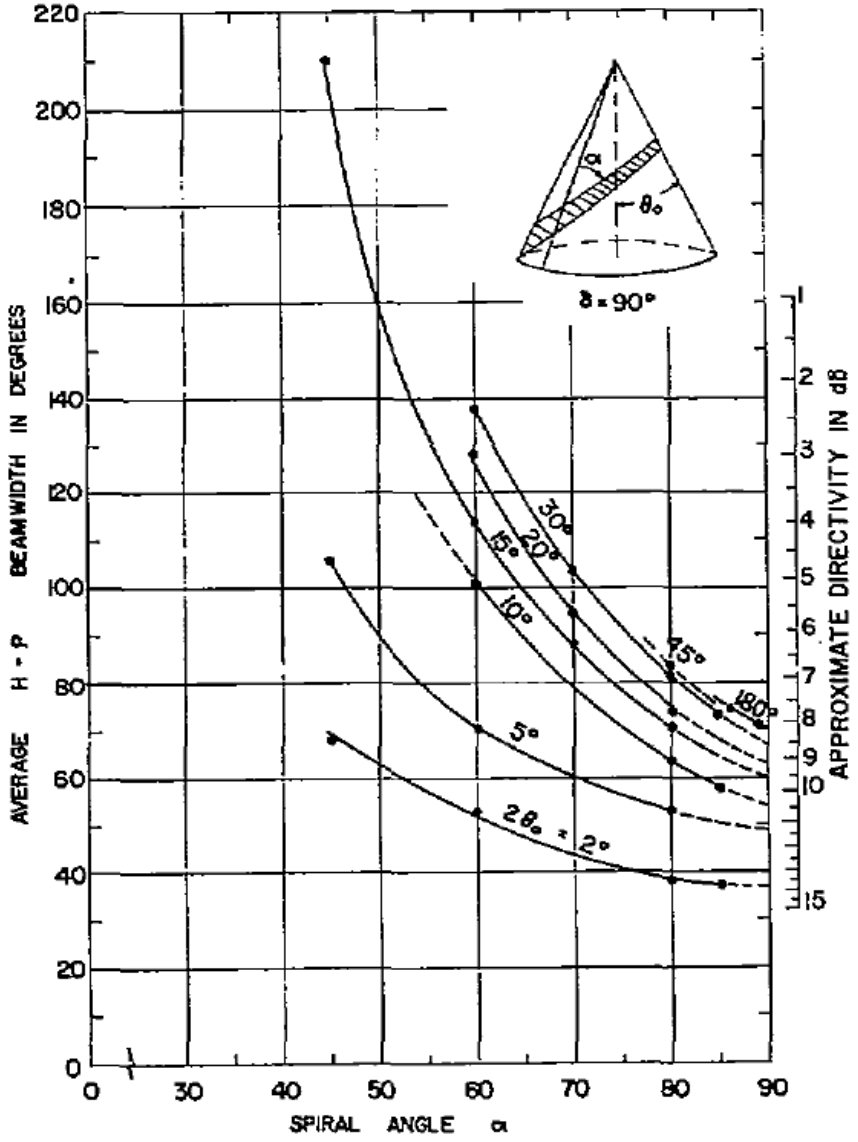

Figure 3.7: Average half-power beamwidth and approximate directivity of the conical log-spiral antennas $\delta = 90^0$ [35]

3.5 Input Impedance of the CLSA

The input impedance of frequency independent antennas is a critical issue. Due to the wide band characteristics of the antenna, it's required to achieve a good impedance matching over a large bandwidth. It is found from the Dyson study that, arm width of the CLSA determines the input impedance. Figure 3.9 shows the variation of the impedance with respect of arms. It is figured out from Dyson experiment that, very small and large width of the arms has impedance of 320π and 80π respectively [35]. The CLSA impedance also influenced by conical angle. Increase in conical angle leads increment of impedance. At highest conical angle

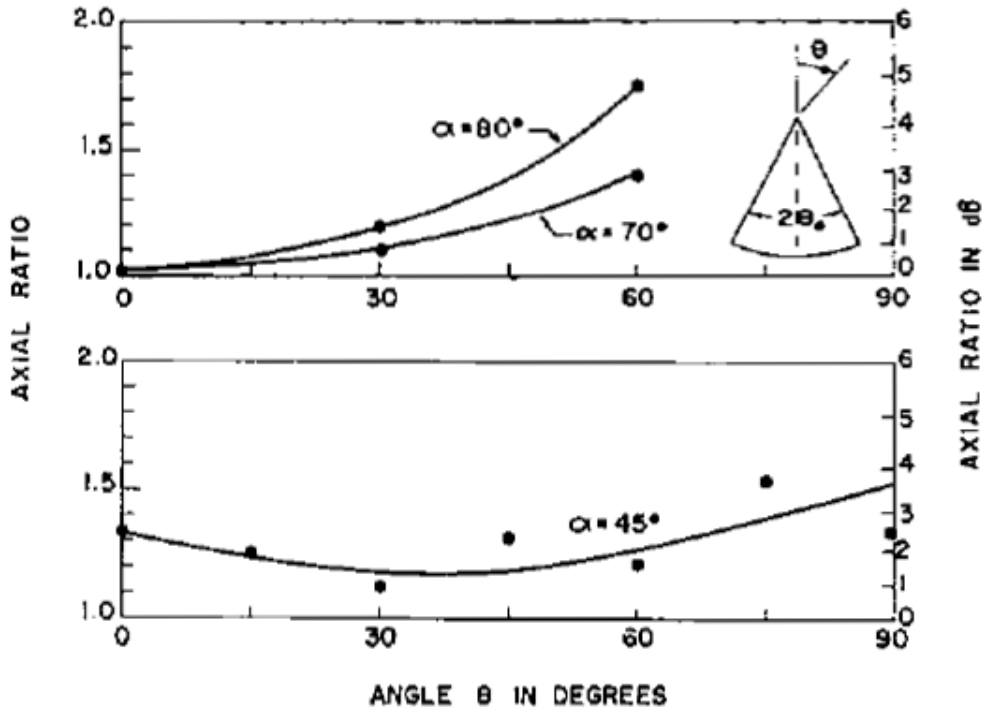

Figure 3.8: Typical axial ratio of the CLSA [35]

which means the amrs are in single plane, the theoretical impedance of the antenna is around 60π or 180π.

3.6 Preliminary Theoretical Design of CLSA

In the previous section of this chapter, the parameters of CLSA is studied according to the Dyson experiment. Based on this study, table 3.1 and table 3.2 are constructed from figure 3.4, which shows the upper and lower radius values in terms of wavelength corresponding to conical and spiral angle. These values are helpful to determine the size of the antenna in terms of radius, height and angle. There are two solutions to identify the lower frequency band. They are ${a_{10}}^{+}$ and ${a_{15}}^{+}$ radii which indicates the lower portion of the active region as discussed in section 3.3. In this case, the portion which is identified by ${a_{10}}^{+}$ is chosen from figure 3.4 to find out the lower edge radius of CLSA in order to achieve compact size of the antenna. Similarly, the upper radius of the antenna can be determined by ${a_{3}}^{+}$ radii which indicates the upper active region and hence using this value we can calculate the radius of the upper cone of the antenna.

Table 3.1 represents the values of upper radius in wavelength for different values of spiral and conical angle and table 3.2 represents lower value of radius in wavelength. In order to achieve the required performance by antenna for the MCA project,

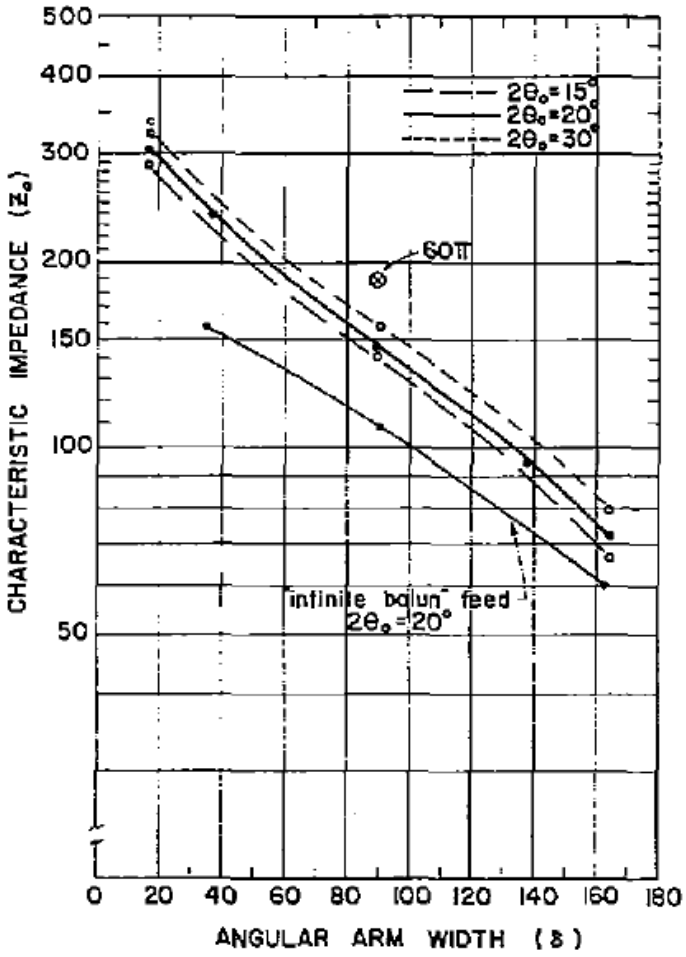

Figure 3.9: characteristics impedance of the CLSA as a function of angular arm width [35]

.

values of spiral and conical angle chose as θ =10° and α =80° respectively. With these values of angle, the HPBW should be 75° with directivity <7 dBi. Now using these values, the upper radius can be calculated by multiplying the upper frequency band with upper radius value, which is taken from table 3.2 and it can be written as

$$r_u = .08\lambda_{\mathrm{u}} = \frac{.08 * c}{f_{\mathrm{u}}} = 1.6mm \tag{3.7}$$

Similarly , lower radius can be calculated by multiplying the lower frequency band with lower radius value, which is taken from table 3.1 and it can be written as

$$r_L = 0.157\lambda_{\mathrm{L}} = \frac{.157 * c}{f_{\mathrm{L}}} = 9.4mm \tag{3.8}$$

Table 3.1: Upper radius values in terms of wavelength for both spiral and conical angles according to Dyson experiment

Spiral Wrap,α	Total conical angle, $2\theta_0$			
	10°	15°	20°	30°
60°	.054	.051	.043	.055
70°	.069	.065	.060	0.056
80°	.089	.083	.079	.070

Table 3.2: Lower radius values in terms of wavelength for both spiral and conical angles according to Dyson experiment

Spiral Wrap,α	Total conical angle, $2\theta_0$			
	10°	15°	20°	30°
60°	0.133	0.146	0.157	0.243
70°	0.130	0.144	0.160	0.183
80°	0.132	0.151	0.157	0.163

Its noticeable from the equation 3.8, that the upper radius is 1.66 mm which is too small. The demerits of having small radius is that, its hard to connect the feed lines through which the antenna is be excited. Moreover, it will be tough to manufacture with very small radius as its required to use advance technology which demands high cost. In order to avoid this problem, the upper radius is selected as 12 GHz instead of 15 GHz which results $r_u = 2$ mm. However, this caused the performance degradation above 12 GHz in terms of HPBW and axial ratio, which is observed in simulation results. This performance degradation in not significant with respect of the MCA project requirements. Hence it is acceptable.

Table 3.3: Design Parameters of CLSA

Design Parameters	Value
Spiral Angle (θ_0)	10°
Conical Angle (θ_0)	80°
Arm width (δ)	$\frac{\pi}{2}$
Upper radius of the cone (r_u)	2 mm
Lower radius of the cone (r_L)	23.5 mm
Initial radial distance (ρ_0)	11.5 mm
Height (H)	124 mm

On the other hand the lower radius is chose 2 GHz in place of 5 GHz, which results $r_L = 23.5$ mm. It is seen from the simulation results that, this value gives better results compare to the radius at 5 GHz. The details theoretical design parameters are

presented in the table 3.3. The CLSA is constructed in CST : Microwave studio using above values and then analyzed the results, which are presented in next chapter.

4 Simulation Process of Conical Log Spiral Antenna

The aim of this chapter is to implement the theoretical model of the CLSA in CST: Microwave studio. A step by step simulation process of the antenna is presented in details. Further, the optimization of CLSA with respect to the MCA project is also described. Finally, the results of simulation in terms of return loss, beam width, input impedance, and axial ratio are displayed and validated with the theoretical values.

4.1 Mapping CLSA Equations in CST

It is mentioned in the previous chapter that, the CLSA is a modification of equiangular spiral as planar form and it must be projected into three dimensions. But the CST simulation domain doesn't has a system for spherical coordinates. Because of this restriction, the equations must be reformulated that are given in chapter 3 for convenient implementation in CST. The new representation form of the CLSA governing equation is as follows:

$$X(u,v); Y(u,v); Z(u,v)$$

Where u and v are parametric variables used for track the function. In equation 3.1, ϕ is responsible for tracing the function. Since there will be no ϕ in reformulated equation, u and v will act as the variable for traces out the equiangular spiral on conical face.

Figure 4.1 shows the cross section of CLSA structure and with the help of this it is possible to find out the starting point of X, Y and Z coordinates. The starting point of X and Y coordinate is related to the upper radius of the cone which can be defined in terms of initial radial distance ρ_0 and it is expressed as:

$$r_u = \rho_0 \sin(\theta_0) \tag{4.1}$$

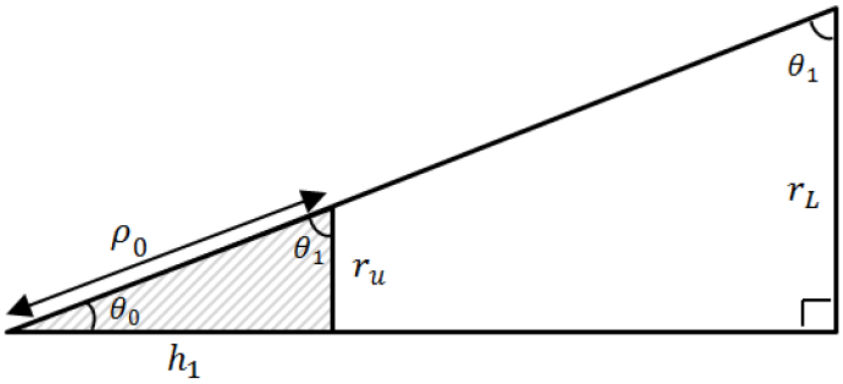

Figure 4.1: Cross section of CLSA structure

.

The way of transformation of the equiangular equation to the parametric equation in CST is to multiply cosine and sine term with X and Y coordinates respectively, which is shown in equation 4.2 and 4.3.

$$X(u,v) = \rho_0 \sin(\theta_0) e^{\beta u} e^{\beta v} \cos(u) = r_u e^{\beta u} e^{\beta v} \cos(u) \tag{4.2}$$

$$Y(u,v) = \rho_0 \sin(\theta_0) e^{\beta u} e^{\beta v} \sin(u) = r_u e^{\beta u} e^{\beta v} \sin(u) \tag{4.3}$$

In above equations, we are familiar with the parameter β and ρ_0 from chapter 3. It is said previously, variable u and v act as a tracing element of the function, where u determines the spiral growth along the cone and v is responsible for variation in wire width respect to spiral growth. To find the starting point of the z coordinate, we can again take the help of figure 4.1 and using geometry it can be written as:

$$h_1 = \rho_0 \sin(\theta_1) \tag{4.4}$$

Where θ_1 is responsible for the starting point of the Z coordinate and using simple geometry it can be written as:

$$\theta_1 = (90^0 - \theta_0) \tag{4.5}$$

Therefore, $Z(u,v)$ can also be expressed the way $X(u,v)$ and $Y(u,v)$ are expressed. Only difference is there will be no sine or cosine terms, because trigonometric function is only required by X and Y coordinates. So $Z(u,v)$ can be written as:

$$Z(u,v) = \rho_0 \sin(\theta_1) e^{\beta u} e^{\beta v} = h_1 e^{\beta u} e^{\beta v} \tag{4.6}$$

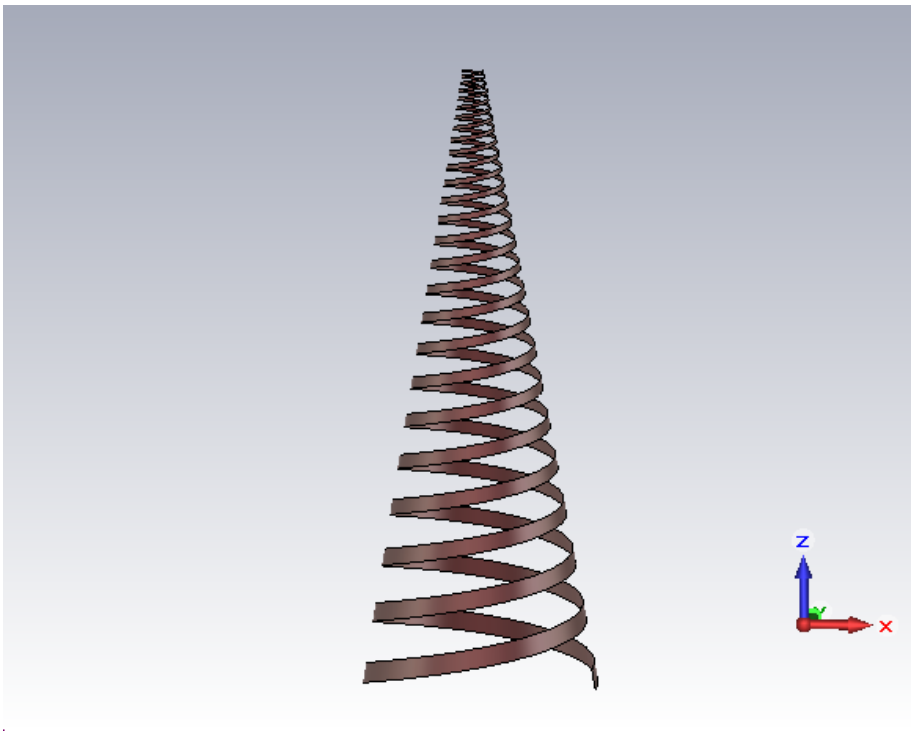

Figure 4.2: Two arm CLSA constructed in CST

.

After reformulation, the next task is to define the range of u and v. The v determines the width of the wire. It should be chosen in a such way that there will be no interference between two neighbouring turns. In addition, as input impedance is greatly influence by the arms width, we should also consider this issue while selecting the range of v. On the other hand, the range of u depends on the angles and the radius of the cone. It can be identified by the smallest point which is starting point and maximum point, where radius of the cone is r_{L}. So it can be represented as:

$$X(u_{max}, v) = r_L = \rho_0 \sin(\theta_0) \mathrm{e}^{\beta u_{max}} \tag{4.7}$$

where $u_{\max}$ can be expressed by rearranging equation 4.1 and 4.7 as follows:

$$u_{max} = ln(\frac{r_L}{\sin(\theta_0)})(\beta^{-1}) \tag{4.8}$$

Thus the scale of u and v can be identified as:

$$u : [0, u_{\max}];\ v : [-width, 0]$$

In order to create a antenna structure in CST, the required parameters has to be chosen. In previous chapter appropriate values of angles are identified from Dyson study. Based on those values, the radius and the range of u and v are calculated theoretically using equations that are derived in this chapter. The next step is to

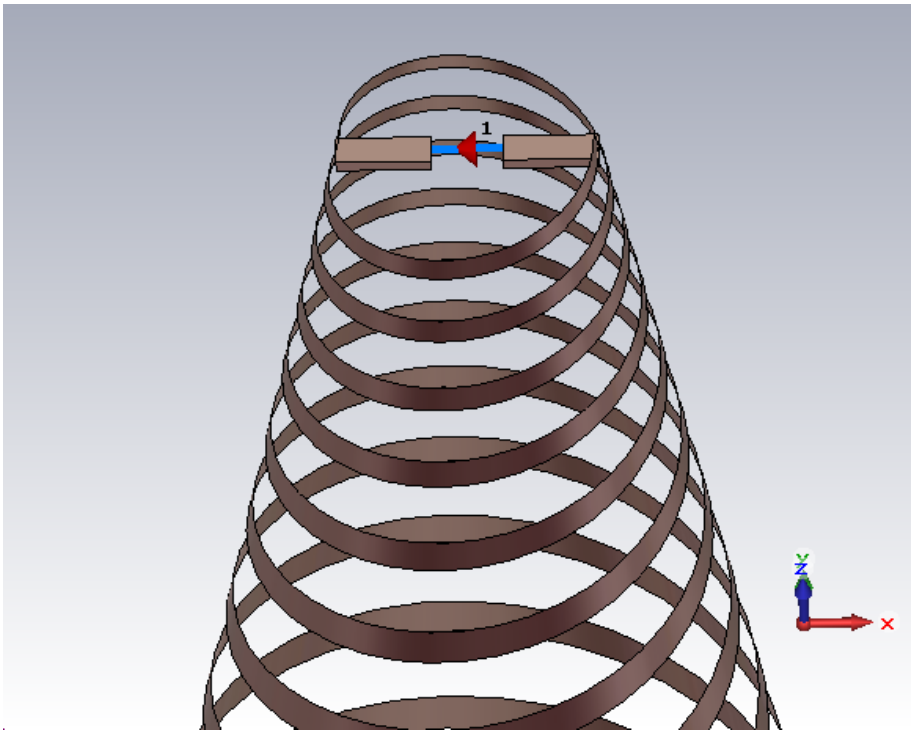

Figure 4.3: CLSA with extending layer and discrete port

.

implement these equations with plugging the calculated values in CST. This will build a CLSA structure with correct dimensions, which will provide our desired outcome.

4.2 Construction of spiral arms and feed

The spiral amrs of the CLSA are created using analytical face tool in CST. All the required equations with proper values are correctly placed in the tool. This will create a single arm CLSA. To obtain double arm, copy of a the same arm is introduced with 180^0 rotation. Figure 4.2 shows a two arm CLSA that is constructed in CST. Once CLSA is constructed, other functionality such as frequency range, cell mashing, simulation accuracy, excitation port, and other necessary functions need to be setup to execute the simulation.

There are two methods to feed the CLSA, which are the top and the bottom feeding. In this case, top feeding is suitable as we want the radiation direction toward the apex of the cone. It is also possible to feed the CLSA at bottom. In that case, the radiation will go backward direction from the apex of the cone and hence other techniques like placing back reflector to redirect the radiation would required, which can make the whole antenna system complex. To feed antenna from the top, a discrete port across the top of the cone to each arms is placed. If the gap between two connection points of the ports is large, then there is a possibility of failing port

definition. To overcome this, the gap is reduced by extending a layer from the top of the arms inward from both sides which is shown in figure 4.3. The width, height, and thickness of the both layers are 0.5 mm, 1.5 mm and 0.2 mm respactively.

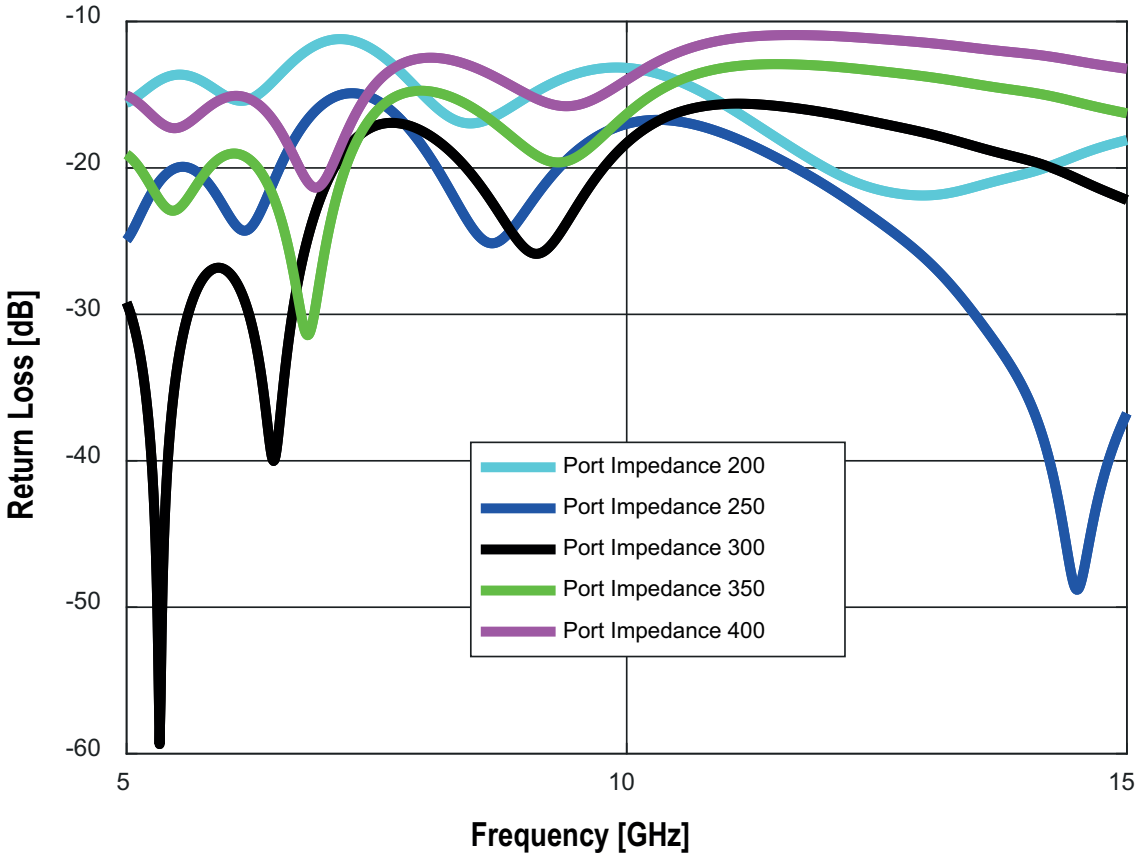

Figure 4.4: Retrun Loss Curve of CLSA for different port impedance's .

.

4.3 Results

In this section, simulation results with optimization are presented. All the results are analyzed based on input impedance, return loss, gain and axial ratio. The simulated results are also validated with the theoretical values.

4.3.1 Return Loss

The target is to achieve below -10 dB return loss which will ensure 90 percent of the incident power is transferred to the antenna. To archive that, best value of input impedance is identified by executing sweep operation in CST. Sweep operation allows to simulate the antenna with different port impedance's at the same time. Figure 4.4 shows the return loss curve for different port impedance's which are simulated with

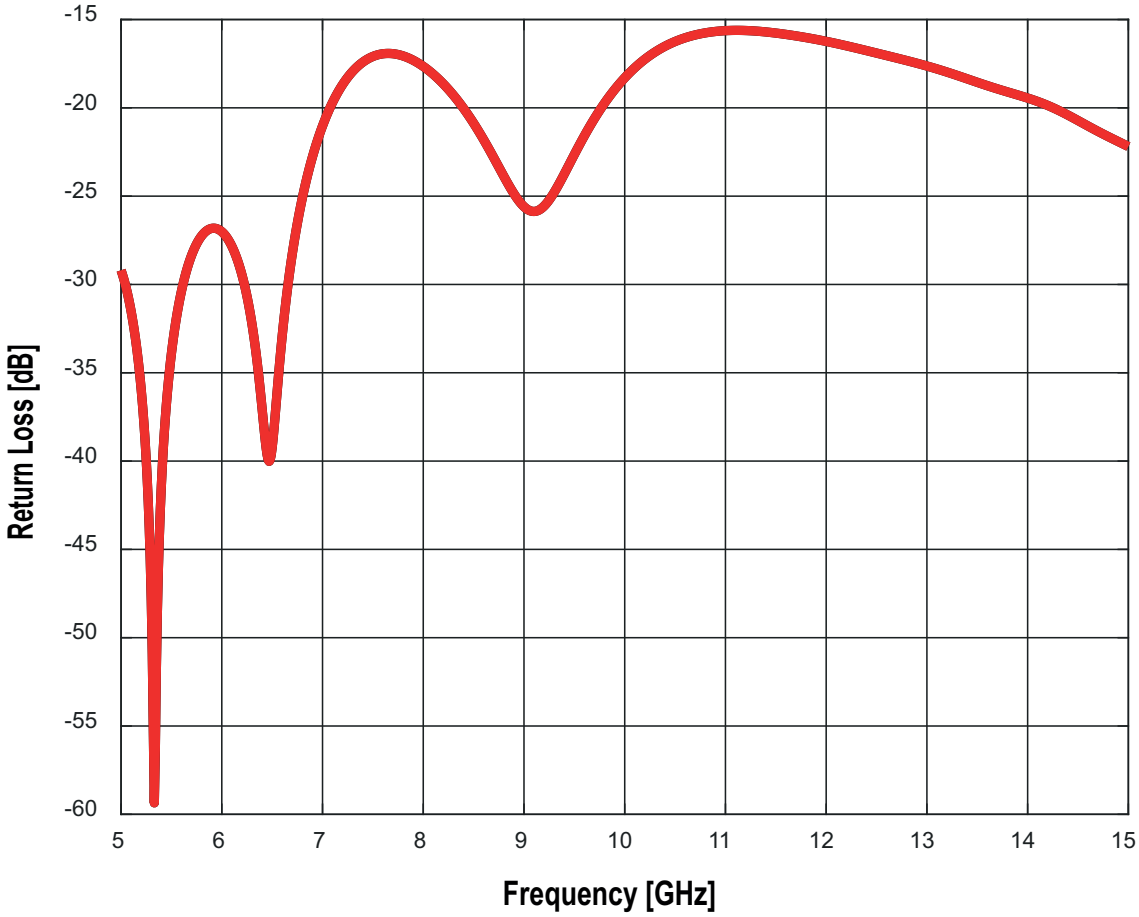

Figure 4.5: Retrun Loss Curve of CLSA at port Impedance 300 Ω.

.

sweep operation. It observed from the curve that, at 200 Ω to 400 Ω port impedance, return loss is below constantly -10 dB over 5 GHz to 15 GHz. Among these, it is found that the impedance matching is best at 300 Ω with practical feeding which is displayed in chapter 5. Figure 4.5 shows the return loss curve at port impedance 300 Ω. Based on this simulation results, the port impedance is chosen as 300 Ω. Thus it can be said that the antenna input impedance is 300 Ω. All the results of other parameters are analyzed at this input impedance.

4.3.2 Far-field Result Analysis

The analysis of radiation pattern of the antenna provides information about gain, directivity, polarization and direction of the radiation. To know the beam width of the antenna, we have to see the polar plots of radiation pattern which is shown in figure 4.6 in the range of 5 GHz to 15 GHz. It is indicating the direction of radiation pattern toward the apex of the cone. This is our desired direction as we fed the antenna from the top of the cone. With the help of Cartesian plots in CST,

beam width of the antenna is calculated at -10 dB level for different frequencies. The significance of taking beam width at -10 dB is discussed in section 2.1.6. Table 4.1 provides the values of beam with at -10 dB for different frequencies. For better visualization, far field 3D radiation pattern is displayed in figure 4.7(a) and 4.7(b).

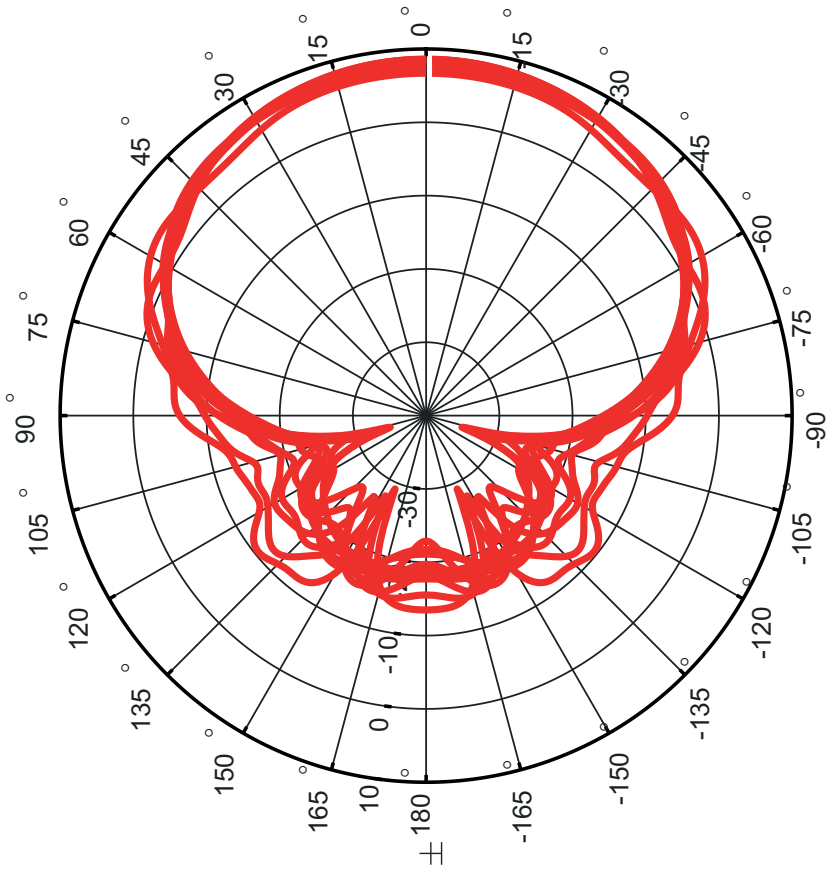

Figure 4.6: Polar plot of the radiation pattern in the range of 5 GHz to 15 GHz with step size 1 GHz.

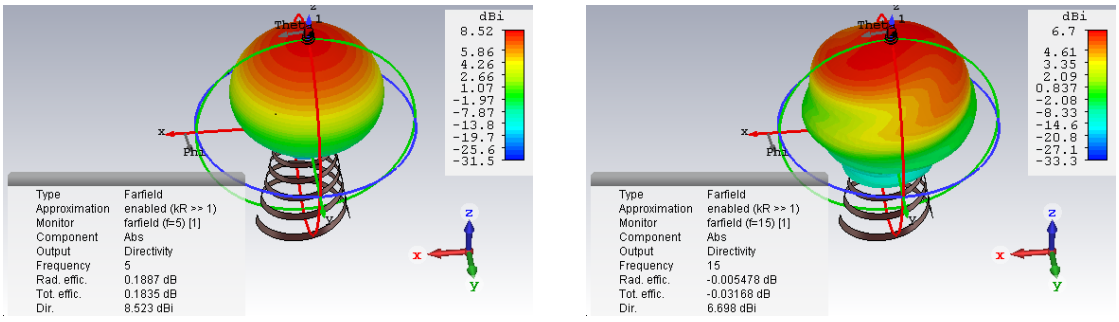

(a) (b)

Figure 4.7: 3D view of the radiation pattern(a) at 5 GHz; (b) at 15 GHz.

Table 4.1: Beam width of CLSA in the range of 5 GHz to 15 GHz with step size 1 GHz.

Frequency (GHz)	HPBW	Beam width (-10 dB level)
5	78°	134°
6	78°	134°
7	78°	134°
8	77°	132°
9	83°	136°
10	78°	130°
11	81°	131°
12	78°	136°
13	79°	140°
14	96°	155°
15	89°	152°

4.3.3 Gain

The gain of the antenna is simulated over 5 GHz to 15 GHz range: The simulation result is found in figure 4.8. We can notice that, the gain is above 7 dBi across the frequency band. In fact, from 5 GHz to 12 GHz, the gain is above 8 dBi and after that its started decreasing. This is because of choosing upper frequency of 12 GHz instead of 15 GHz. As it is discussed in chapter 3 , the upper frequency is chosen 12 GHz to increase the upper radius of the cone so that its large enough to realize practically. As a consequence, the performance is degraded after 12 GHz. However, its is acceptable as the gain of the parabolic reflector is increase with the increase of frequency [37].

4.3.4 Axial Ratio

To realize the polarization state of the antenna, analysis of axial ratio need to be done. One of the key goal of this thesis is to design a circular polarized antenna. The important of the circular polarization is discussed in section 2.1.8. The axial ratio is simulated through out the frequency range and its found below 3 dBi at maximum radiation direction shown in the figure 4.9. Therefore, it is clearly indicating the antenna is circular polarized.

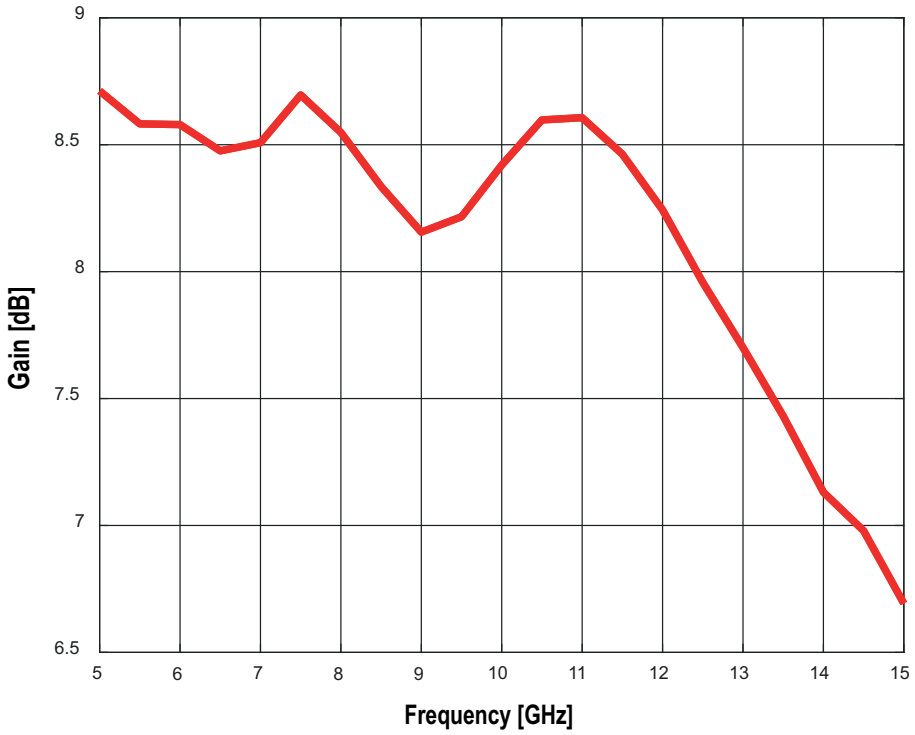

Figure 4.8: Gain of the Simulated CLSA

.

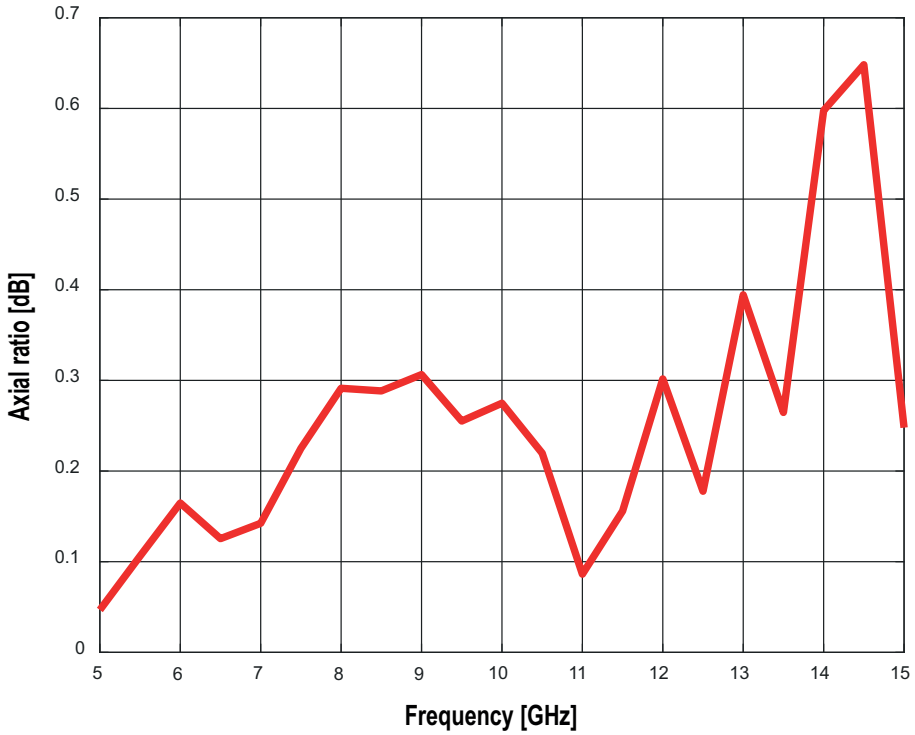

Figure 4.9: Axial Ratio of the Simulated CLSA

.

4.4 Results Conclusions

The simulation results shows a good agreement to the theoretical values. The impedance of the antenna is well matched across the frequency band which indicates that, most of the power is transferred to the antenna. According to the theoretical study, the gain should be <7 dBi. The simulation results reflects the same outcome, in fact its <8 dBi but its starts decreasing after 12 GHz though its still remain almost above 7 dBi. Similarly, simulated HPBW is in between 60° to 80° for whole frequency band, which is expected value as theoretical study also suggested same. Most noticeable point is that, the beam width is almost constant across the frequency band and its a significant results as the MCA project strongly demands a constant beam width from the feed. The axial ratio also follows the theoretical outcome. It is found below 3 dB across the frequency range. This means the antenna is circular polarized which is one of the main characteristics of the conical log spiral antennas.

5 Feeding Methods and Mechanical structure of CLSA

The feeding of CLSA is a challenging task. This chapter is focused on feeding strategies of the CLSA. In addition, other components related to the feed of the antenna are analyzed. Moreover, guidelines for mechanical structure in order to provide stable support to the antenna are provided.

5.1 Bifilar Lines

It is discussed in previous chapter that, the CLSA with top feeding is suitable for this work. The problem of feeding the antenna from the top is that, some kind of connection is required to supply energy form the source for practical implementation. That means a practical feeding procedure is required to excite the antenna. In this case, bifilar lines can be a promising solution. Bifilar lines are made of two conductors, separated by a dielectric. which shown in figure 5.1.

Figure 5.1: Geometry of Bifilar Lines

.

The advantage of using bifilar line is that, it is possible to choose the impedance of it easily according to the application. Thus it is very convenient to use. Moreover, design of the bifilar line is aslo very simple. The mathematical expression for finding out the impedance of the bifilar lines can be written as:

$$Z_0 = \frac{276}{\sqrt{k}} \log_{10} \frac{d}{r} \tag{5.1}$$

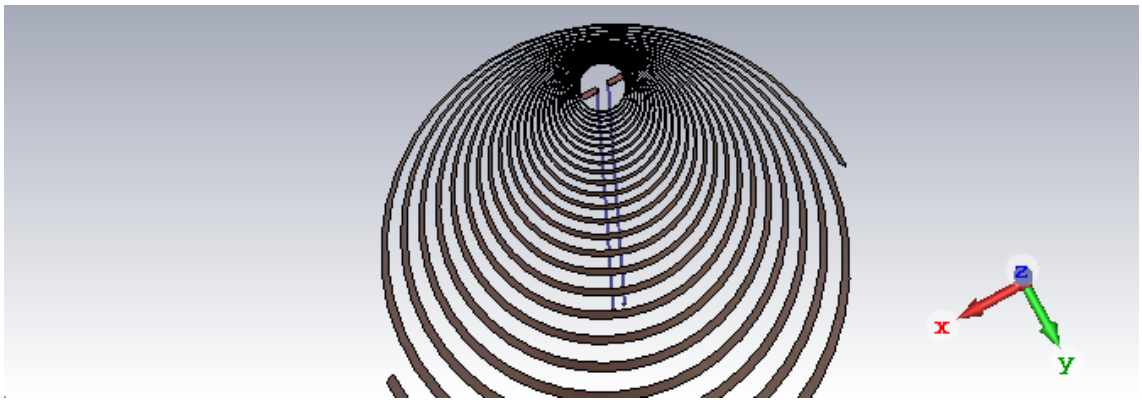

Figure 5.2: Top view of CLSA with bifilar lines

.

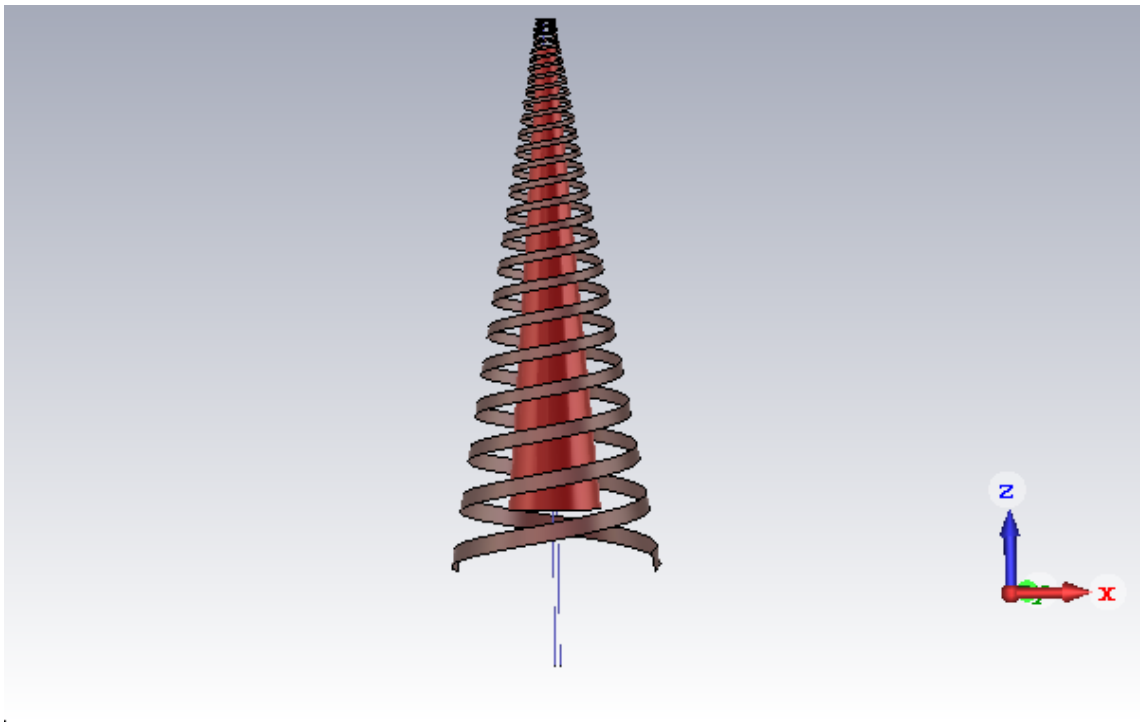

Figure 5.3: CLSA with bifilar lines and Hollow metal

.

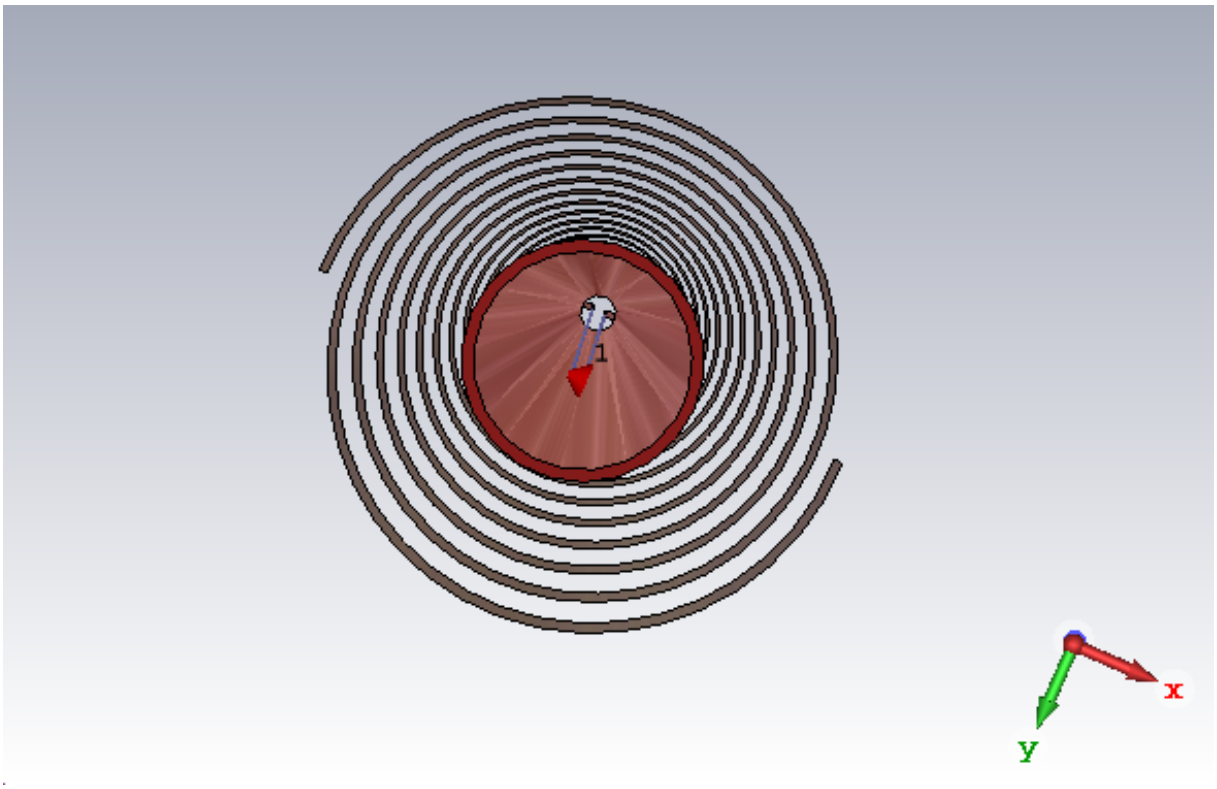

Figure 5.4: Bottom view of CLSA with bifilar lines and hollow metal

.

where k is dielectric constant which is air in this case, Z_0 is charateristics impedance of the lines, r is the radius of the conductors and d is the separation distance between two conductors. The CLSA with bifilar lines is shown in figure 5.2. Using this equation, the radius $r = .33$ mm and the separation distance $d = 1$ mm are chosen at characteristics impedance 300 Ω. It is found after optimization, the radius $r = .15$ mm with distance $d = 1$ mm gives better performance at antenna input impedance 300 Ω.

5.2 CLSA Performance with Bifilar Lines

It is figured from the simulation results that, the antenna performance degraded in terms of radiation pattern with bifilar lines. This is because the bifilar lines also radiates energy which overlapped with the main radiation destructively. As a results, the radiation pattern performance gets worse. To avoid this issue, a hollow metal is inserted inside the antenna which covers the bifilar lines without touching the lines and the antenna, which is dispalyed in figure 5.3. That means the hollow metal is free from both the antenna and the bifilar lines.

For the better understanding of physical structure of the bifilar lines and the hollow metal, a bottom view of CLSA is presented in figure 5.4. The consequences of this

technique is that, the waves that are coming from the bifilar lines are reflecting back from the high conductive hollow metal and hence the energy that is coming from the bifilar line is not going out from the hollow metal. As the inserted hollow metal is free, its not radiating any energy by it self. However, there are some radiation due to mutual coupling between bifilar lines and hollow metal but the strength of this radiation is not so much that can harm the main radiation significantly.

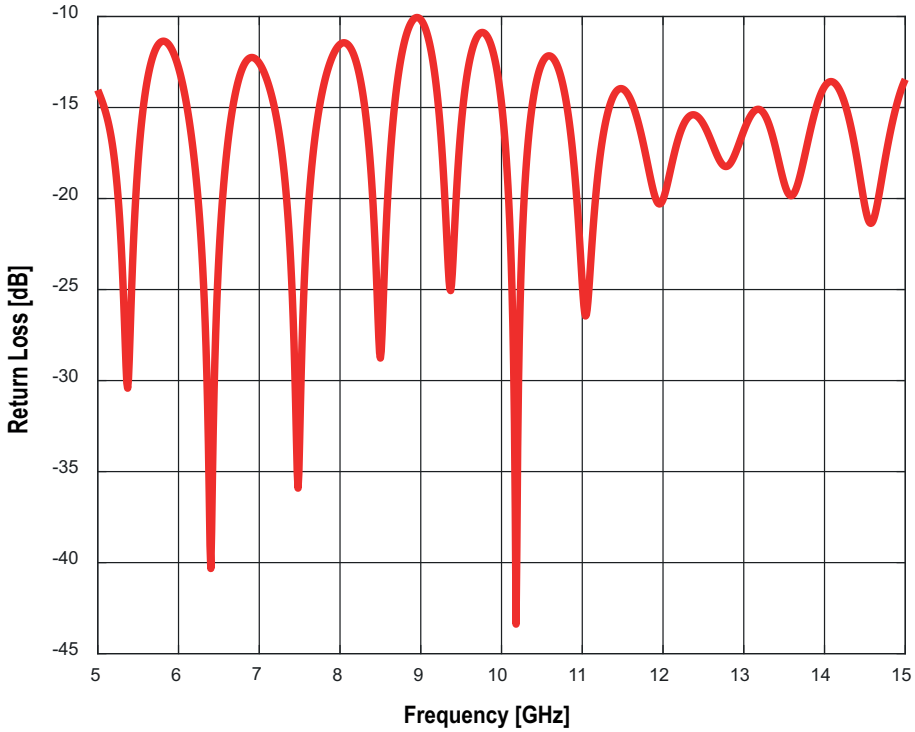

Figure 5.5: return loss of the Simulated CLSA with bifilar lines and Hollow metal

.

Figure 5.5, 5.6, and 5.7 shows the simulation results of CLSA with bifilar lines and hollow metal in terms of return loss, gain, and axial ratio respectively. The results indicates that, performance of the CLSA with bifilar lines and hollow metal degraded compared to without lines and hollow metal. This consequence points out that, there are still some radiation coming out from the bifilar lines which are harming the main radiation. But in this case, the strength of the radiation is not so powerful that can destroy the main radiation significantly. With the practical feeding, the gain of the antenna decreases. but still its above 7 dBi at most of the frequencies. However, at some frequencies the gain is little bit below 7 dBi. For example, at 8.5 GHz, 14 GHz and 13 GHz, the gain is below 7 dBi. The axial ratio shows good performance and it below 3 dB across the frequency range though its performance degraded compare to CLSA without lines and hollow metal. But it is not remarkable at all.

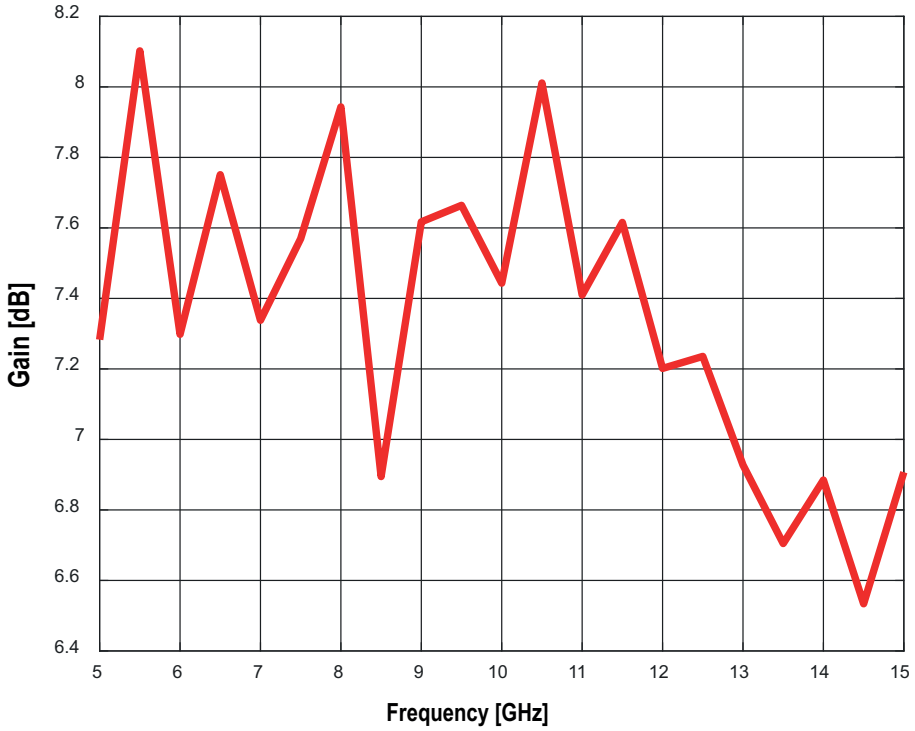

Figure 5.6: Gain of the Simulated CLSA with bifilar lines and Hollow metal

.

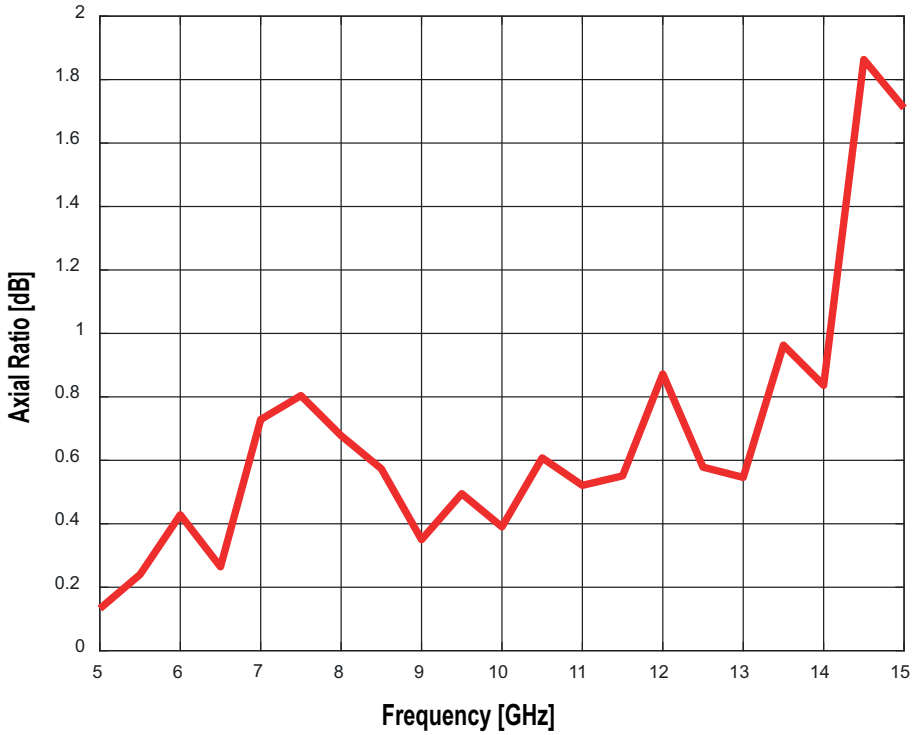

Figure 5.7: Axial ratio of the Simulated CLSA with bifilar lines and Hollow metal

.

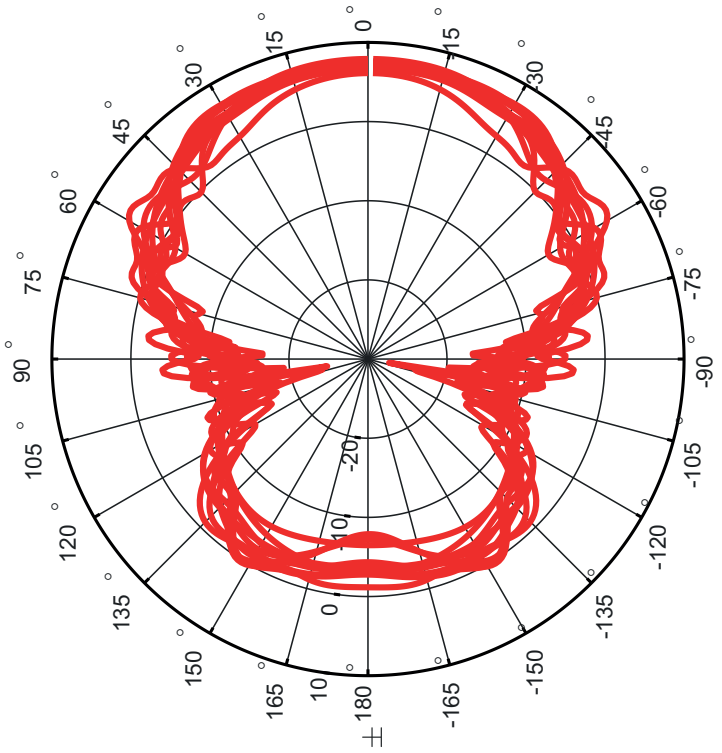

Figure 5.8: Polar plots of the radiation pattern with biflar lines and hollow metal in the range of 5 GHz to 15 GHz with step size 1

.

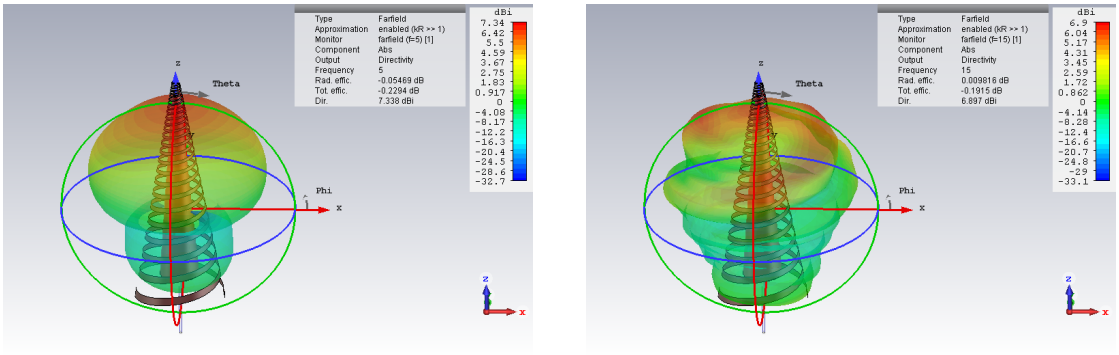

(a) (b)

Figure 5.9: 3D view of the radiation pattern(a) at 5 GHz; (b) at 15 GHz.

On the other hand, the radiation pattern is degraded which can be realized from the polar plots shown in figure 5.8. The HPBW is higher in every cases compare to normal feeding except at 14 GHz and 15 GHz . As a result, the gain is decreased across the frequency band. Although its still above 7 dBi in most of the frequencies. However, beam width at -10 dB level is constant across the frequency range but in some instances it is less then the requirements, which is still acceptable. Table 5.1

provides the values of HPBW and beam width at -10 dB level which is constructed using the help of Cartesian plots of radiation pattern. It can be notice that, in some cases the values for HPBW vs -10 dB level beam width is quite different. This is because the beam shape distorted little bit due to the overlapping of the waves between the bifilar lines and the antenna. For better realization, 3D Plots of radiation pattern at 5 Ghz and 15 GHz is shown in the figure 5.9(a) and 5.9(b).

Table 5.1: Beam width of CLSA with bifilar lines and hollow metal in the range of 5 GHz to 15 GHz with step size 1 GHz.

Frequency (GHz)	HPBW	Beam width (-10 dB level)
5	90°	155°
6	93°	140°
7	64°	152°
8	80°	138°
9	88°	152°
10	84°	146°
11	90°	154°
12	88°	145°
13	77°	160°
14	52°	152°
15	52°	142°

5.3 Balun

To connect the antenna to the reciver and energy source, other components such as balun and low noise amplifier (LNA) is required. Block diagrams are presented to realize the total antenna and receiver system which shows different parts of the system. Figure 5.10 shows the total antenna system in telescope uses and 5.11 shows the total antenna system in performance testing.

Figure 5.10: Block Diagram of the total antenna system in telescope usages

.

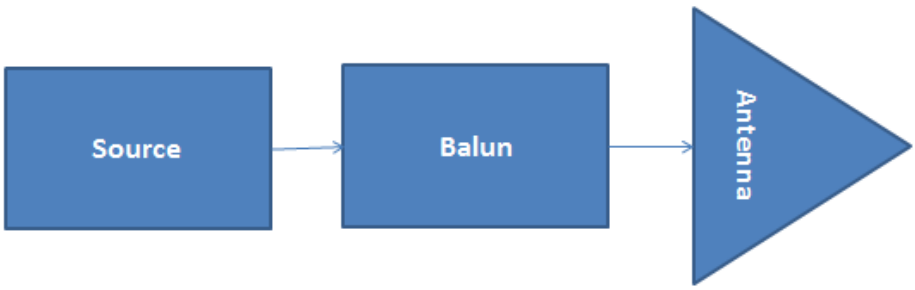

Figure 5.11: Block Diagram of the total antenna system in performance testing

.

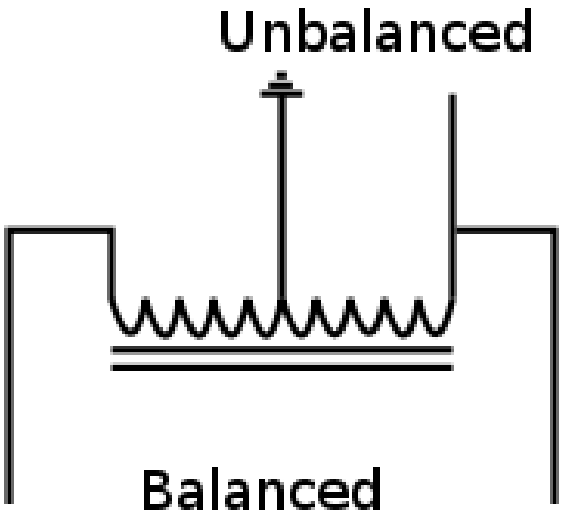

Figure 5.12: Typical schematic of a balun

.

It is mentioned in previous chapter that, the CLSA is a balanced structure. That means both of the arms carries same current but in opposite direction. On the other hand, conventional transmission lines are unbalanced. Because of that, a transformer is needed for converting the unbalance line to the balance line. Furthermore, conventional lines has a standard values of impedance which are mostly 50 Ω and 75 Ω. Because of that, a impedance transformer is also required. To master these problems, a balun could be a favourable solution. A balun is a device which can transfer the balanced line to the unbalance line or vice versa. Besides it can also be a impedance transformer. Figure 5.12 shows a typical scematic of balun. Depending on the application, the type of balun is selected. For CLSA, a transformer type balun is necessary which can work as a impedance transformer as well as a converter for the unbalance line to the balance line.

The balun can be found commercially in the market but they have some standard specifications. Due to that, most of the time balun need to be designed according to the application requirements. As it is required to choose suitable input impedance of the antenna for better performance, it would be wise thing to design a balun for CLSA rather then using commercial one. For designing such kind of balun for the CLSA, further study on it is essential.

5.4 Mechanical Structure

One of the key requirement of the MCA is to have a rugged construction of the antenna. The dishes that has been donated to the MRO are parabolic dish and the feed system is focal feed which is also known as front feed system. The designed antenna of this thesis work is to be use as a feed for one of the donated dish antenna. The geometry of this dish antenna is shown in figure 5.13. We can see from the geometry that, the antenna needs to be placed in the focal point in order to get the front feed system. Since the dish antenna is located in outside environment, the mechanical structure and support of the antenna should be strong and robust. There could be many possible way to design the mechanical support structure of the antenna. One of the way is shown in the figure 5.14.

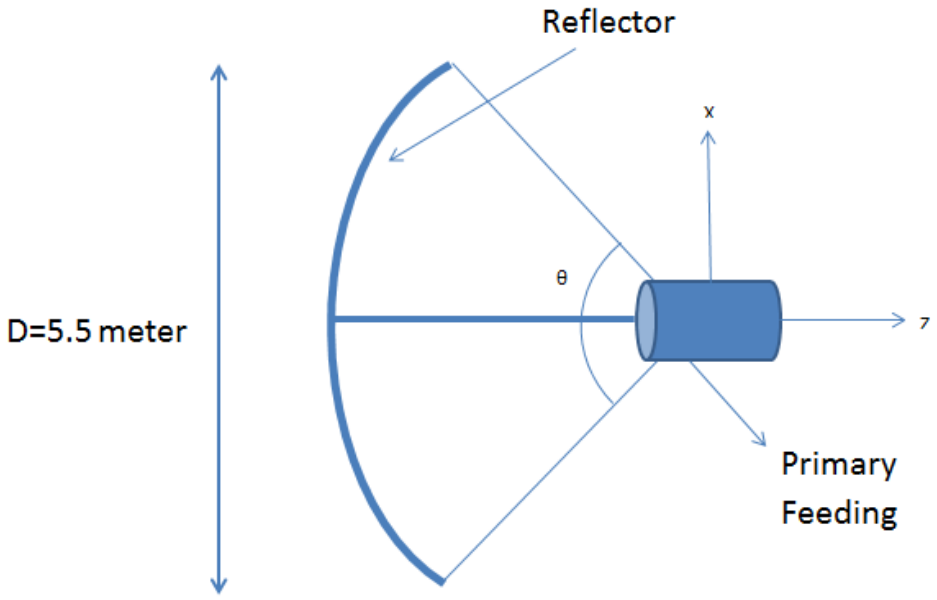

Figure 5.13: Geometry of a donated parabolic dish

In this figure, a cylindrical structure having radius and height of 25 mm is considered. The material of the the structure could be a metal or plastic. It has no significance to antenna performance as it does not has any direct physical connection with the antenna. The arms of the antenna is connected to the cylindrical structure via

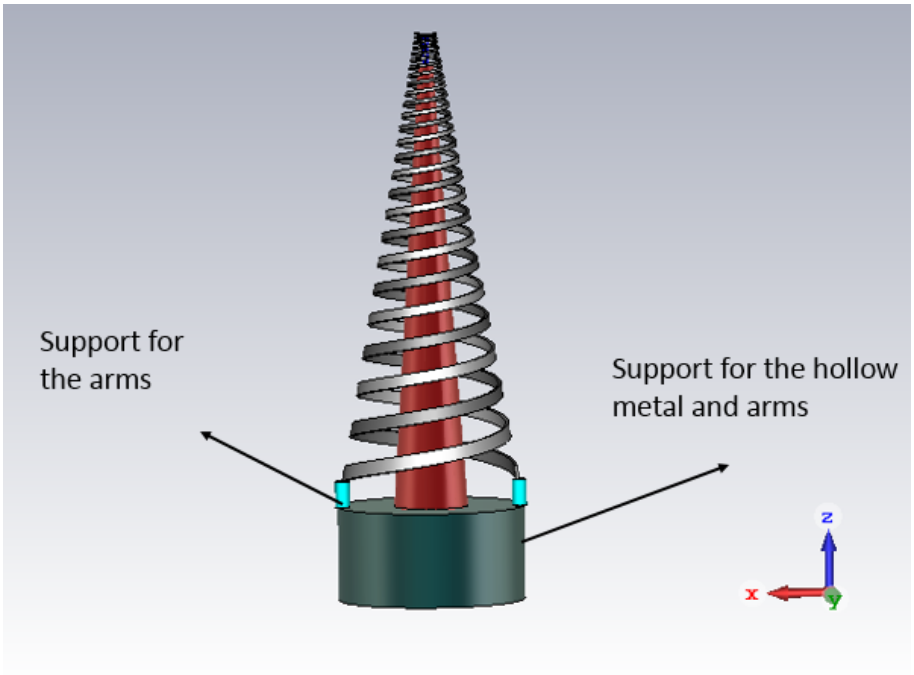

Figure 5.14: CLSA with mechanical support stucture

another cylindrical supports, which has radius of 2 mm and height of 7 mm. This cylindrical support has to be a non conducting materiel, otherwise the support structures will get excited by the antenna, which can destroy the performance of the antenna.

6 Conclusions

In this master thesis, a two arm conical log spiral antenna is analyzed and designed as a reflector feed for achieving the set up goal of the MCA project. First, the antenna is designed theoretically based on the Dyson study and developed design equations of the antenna using the theory of equiangular spiral antenna. Moreover, the design equations are reformulated in order to construct and simulate the antenna in CST. The simulation results shows a very good harmony to the theoretical values in terms of return loss, bandwidth, gain, and axial ratio. Besides, the antenna is investigated with the bifilar line to realize the feeding of the antenna practically but the results was worse due to the overlapping between the radiations coming from the bifilar line and the antenna. The concept of inserting a hollow metal to cover the bifilar line in order to block the radiation of the bifilar line is presented. The simulation results of the antenna with bifilar line and hollow metal exhibits fair performance which fulfils most of the requirements that has set up for this work. Furthermore, the guidelines for mechanical support and structure of the antenna to have rugged construction and protection from outside environment is presented. In addition, one possible mechanical structure is designed and displayed in CST.

Future works includes, the fabrication of the antenna and the experimental investigation to validate the simulation results. It is found from this study that, the top feeding is more affective and suitable compare to the bottom feeding although it is hard to realize the top feeding as the radius of the the upper cone of the antenna is very small. More investigation on feeding strategies can be done to achieve simple and convenient way to excite the antenna. In that case, optimization of the antenna might be required to make an adjustment with the new feeding method. As the antenna structure is a balanced system, details study on balun must be done to design the balun specifically for this antenna. The designed antenna can provide either RHCP or LHCP depending on the direction of the spiral growth. To get the dual polarization, array of two or more elements need to be considered. Further, study on mechanical structure of the antenna should be done in order to achieve easy and more rugged construction compare to the current one.

References

[1] P. L. McMahon, "Adventures in radio astronomy instrumentation and signal processing," M.S thesis, University of Cape Town, 2008.

[2] J. P. P. WEEM, "Broad band antenna arrays and noise coupling for radio astronomy," Doctoral thesis, University of Colorado, 1996.

[3] "Private discussion with dr. joni tammi, director, elec/metsähovi radio observatory."

[4] V. Rumsey, "Frequency independent antennas," in *IRE International Convention Record*, vol. 5, March 1957, pp. 114–118.

[5] V.Rumsey, *Frequency independent antennas.* NY, USA: Academic Press, 1966.

[6] J. Dyson, "The equiangular spiral antenna," *IRE Transactions on Antennas and Propagation*, vol. 7, no. 2, pp. 181–187, April 1959.

[7] J.Dyson, "The unidirectional equiangular spiral antenna," *IRE Transactions on Antennas and Propagation*, vol. 7, no. 4, pp. 329–334, October 1959.

[8] E. C. Jordan, G. A. Deschamps, J. D. Dyson, and P. E. Mayes, "Developments in broadband antennas," *IEEE Spectrum*, vol. 1, no. 4, pp. 58–71, April 1964.

[9] R. Wills, "A submarine multifunction antenna," *Communication Broadcasting*, vol. 9, no. 3, p. 39–45, 1985.

[10] P. A. Ramsdale and P. W. Crampton, "Properties of 2-arm conical equiangular spiral antenna over extended bandwidth," *Microwaves, Optics and Antennas, IEEE Proceedings H*, vol. 128, no. 6, pp. 311–316, December 1981.

[11] "Cst - computer simulation technology." [Online]. Available: https://www.cst.com.

[12] H. J. A. Giselle M. Galvan-Tejada, Marco Antonio Peyrot-Solis, *Ultra Wideband Antennas: Design, Methodologies, and Performance.* NY, USA: CRC Press, 2015.

[13] R. R. Ramirez and N. G. Alexopoulos, "Single proximity feed microstrip archimedean spiral antennas," in *IEEE Antennas and Propagation Society International Symposium. 1998 Digest. Antennas: Gateways to the Global Network. Held in conjunction with: USNC/URSI National Radio Science Meeting (Cat. No.98CH36*, vol. 2, June 1998, pp. 664–667 vol.2.

[14] D. R. Ribeiro, L. A. de Santana, M. C. Alves, J. F. Almeida, and C. L. da S. S. Sobrinho, "Spiral microstrip antenna," in *2007 SBMO/IEEE MTT-S International Microwave and Optoelectronics Conference*, Oct 2007, pp. 104–106.

[15] M. F. A. Khalid, M. A. Haron, A. Baharudin, and A. A. Sulaiman, "Design of a spiral antenna for wi-fi applications," in *2008 IEEE International RF and Microwave Conference*, Dec 2008, pp. 431–435.

[16] Z. H. Changjie Sun, Guobin Wan and X. Ma, "Design and simulation of planar archimedean spiral antenna," in *2008 IEEE International RF and Microwave Conference*, 1998.

[17] C. Balanis, *Antenna Theory: Analysis and Design, 3rd ed.* NY, USA: Jhon willey and sons, 2005.

[18] K. Louertani, N. Ribiere-Tharaud, R. Guinvarc'h, and M. Helier, "Coplanar feeding solution for spiral antenna," in *2009 IEEE Antennas and Propagation Society International Symposium*, June 2009, pp. 1–4.

[19] D. King, R. Packard, and R. Thomas, "Unequally-spaced, broad-band antenna arrays," *IRE Transactions on Antennas and Propagation*, vol. 8, no. 4, pp. 380–384, July 1960.

[20] Y. Lo, "A mathematical theory of antenna arrays with randomly spaced elements," *IEEE Transactions on Antennas and Propagation*, vol. 12, no. 3, pp. 257–268, May 1964.

[21] R. DuHamel and D. Isbell, "Broadband logarithmically periodic antenna structures," in *1958 IRE International Convention Record*, vol. 5, March 1957, pp. 119–128.

[22] R. DuHamel and F. Ore, "Logarithmically periodic antenna designs," in *1958 IRE International Convention Record*, vol. 6, March 1958, pp. 139–151.

[23] D. G. Shively and W. L. Stutzman, "Wideband arrays with variable element sizes," *IEE Proceedings H - Microwaves, Antennas and Propagation*, vol. 137, no. 4, pp. 238–240, Aug 1990.

[24] J. Thaysen, K. B. Jakobsen, and H. R. Lenler-Eriksen, "Wideband cavity backed spiral antenna for stepped frequency ground penetrating radar," in *2005 IEEE Antennas and Propagation Society International Symposium*, vol. 1B, 2005, pp. 418–421 vol. 1B.

[25] J. Volakis, *Antenna Engineering Handbook 4th Ed.* NY, USA: McGraw-Hill, 2007.

[26] H. Nakano, T. Igarashi, H. Oyanagi, Y. Iitsuka, and J. Yamauchi, "Unbalanced-mode spiral antenna backed by an extremely shallow cavity," *IEEE Transactions on Antennas and Propagation*, vol. 57, no. 6, pp. 1625–1633, June 2009.

[27] S. Hong, J. Lee, and J. Choi, "Design of a novel modified spiral antenna for uwb application," in *2008 Asia-Pacific Microwave Conference*, Dec 2008, pp. 1–4.

[28] J. P. P. WEEM, "Soiral slot antenna," Doctoral thesis, Wright air development centre, Dyton, june, 1995.

[29] L. Schreider, X. Begaud, M. Soiron, and B. Perpere, "Archimedean microstrip spiral antenna loaded by chip resistors inside substrate," in *IEEE Antennas and Propagation Society Symposium, 2004.*, vol. 1, June 2004, pp. 1066–1069 Vol.1.

[30] P. C. Werntz and W. L. Stutzman, "Design, analysis and construction of an archimedean spiral antenna and feed structure," in *Southeastcon '89. Proceedings. Energy and Information Technologies in the Southeast., IEEE*, Apr 1989, pp. 308–313 vol.1.

[31] M. N. M. Tan, S. K. A. Rahim, M. T. Ali, and T. A. Rahman, "Smart antenna:weight calculation and side-lobe reduction by unequal spacing technique," in *2008 IEEE International RF and Microwave Conference*, Dec 2008, pp. 441–445.

[32] W.-Z. Wu, T.-H. Chang, and J.-F. Kiang, "Broadband slot spiral antenna with external feed and microstrip-to-slot line transition," in *IEEE Antennas and Propagation Society Symposium, 2004.*, vol. 1, June 2004, pp. 767–770 Vol.1.

[33] M. W. N. Dejan S. Filipovic1, Thomas P. Cencich2, *Frequency independent antennas.* Wiley Online Library, 2005.

[34] A. J. Ernest, Y. Tawk, J. Costantine, and C. G. Christodoulou, "A bottom fed deployable conical log spiral antenna design for cubesat," *IEEE Transactions on Antennas and Propagation*, vol. 63, no. 1, pp. 41–47, Jan 2015.

[35] J. Dyson, "The characteristics and design of the conical log-spiral antenna," *IEEE Transactions on Antennas and Propagation*, vol. 13, no. 4, pp. 488–499, Jul 1965.

[36] T. W. Hertel and G. S. Smith, "The conical spiral antenna over the ground," *IEEE Transactions on Antennas and Propagation*, vol. 50, no. 12, pp. 1668–1675, Dec 2002.

[37] T. A. Milligan, *Modern antenna design, 2nd Edition.* New Jersey, USA: A Jhon Willy Sons, INC., Publication, 2005.